Doctoral dissertation

University of Szeged
Faculty of Pharmacy
Department of Pharmaceutical Technology
Head: Prof. Dr. Habil. István Erős Ph.D., D.Sc.

NEW POSSIBILITIES FOR THE DEVELOPMENT OF IRON(II) SULFATE CONTAINING SOLID PRODUCTS WITH SUSTAINED DRUG RELEASE

By
Edina Pallagi
Pharmacist

Supervisors:
Prof. Dr. Révész Piroska
University of Szeged, Department of Pharmaceutical Technology
Prof. Dr. Joachim Ulrich
Martin-Luther University, Halle-Wittenberg, Department of Process Engineering

Szeged
2004

Publications

I. T. Haasner, J. Ulrich, ***E. Pallagi***, P. Szabó-Révész: Kugeln ohne Kanten, Einfluss der Oberflächen-eigenschaften auf die Tropfenerstarrung von Schmelzen auf festen Oberflächen, *Verfahrenstechnik 35 (2001), 34-39.*

II. ***Pallagi E.***, Szabóné Révész P., Erős I.: A nedvesedési szög és a felületi szabad energia meghatározásának elmélete és gyakorlata, *Gyógyszerészet, 47 (2003) 83-90.*

III. Laczkovich O., Révész P., ***Pallagi E.***, Erős I.: Vas(II)-szulfát hőstabilitásásnak vizsgálata gyógyszer-formulálási céllal, *Acta Pharmaceutica Hungarica, 73 (2003) 243-248.*

IV. ***E. Pallagi***, P. Szabó-Révész, T. Haasner, M. Pásztor-Turák, O. Laczkovich, J. Ulrich, I. Erős: Entwicklung von Eisen(II)-sulfat-enthaltenden Einbettungspartikeln, *Pharm. Ind. 66 (2004) 112-117.*(IF: 0,279)

V. ***E. Pallagi***, K. Vass, K. Pintye-Hódi, P. Kása Jr., G. Falkay, I. Erős, P. Szabó-Révész, Iron(II) sulfate release from drop-formed lipophilic matrices developed by special hot-melt technology, *Eur. J. Pharm. Biopharm. 57/2 (2004) 287-294.* (IF: 2,064)

VI. ***Pallagi E.***, Szabóné Révész P., Erős I.: Amit a vasról és a vastartalmú készítményekről tudnunk kell, *Gyógyszerészet, 48 (2004) 332-338.*

VII. ***E. Pallagi***, P. Szabó-Révész, J. Ulrich, I. Erős: Use of glycerine derivatives in melt solidification for the development of iron(II) sulfate-containing particles, *Journal of Drug Delivery Science and Technology (STP Pharma Sciences)* (In Press.).

VIII. P. Szabó-Révész, B. Farkas, ***E. Pallagi***, K. Nagy, I. Erős: Spherical crystallization of iron(II) sulfate heptahydrate for development of solid dosage form, *Pharm. Research.* (In Press.)

Abstracts

I. ***Pallagi E.***: Vas(II)-szulfát tartalmú pelletek elõállítása olvadékból történõ konfekcionálással, *TDK-Konferencia, Szeged, 2001. febr. 15-17.*

II. ***Pallagi E.***: Vas(II)-szulfát tartalmú pelletek elõállítása olvadékból történõ konfekcionálással, *Országos TDK-Konferencia, Pécs, 2001. ápr. 4-7.*

III. ***Pallagi E.***: Vas(II)-szulfát tartalmú szemcsék fejlesztése speciális olvadéktechnológia alkalmazásával, *VI. Clauder Ottó Emlékverseny, Budapest, 2002. szept. 26-28.*

IV. ***Pallagi E.***: Szabóné Révész P., Vass K., Hódi K., ifj. Kása P., Falkay Gy., Erős I., Vas(II)-szulfát tartalmú szemcsék in vitro és in vivo összehasonlító vizsgálata, *XIV. Országos Gyógyszertechnológiai Konferencia, Hévíz, 2002. nov. 8-10.*

V. P. Szabó-Révész, ***E. Pallagi***, K. Vass, K. Pintye-Hódi, J. Ulrich, G. Falkay, I. Erős: Development of iron(II) sulfate containing dropformed pastilles with special hot melt technology, *4th World Meeting on Pharmaceutics, Biopharmaceutics and Pharmaceutical Technology, 8-11. Apr. 2002., Florence, Italy*

VI. ***E. Pallagi***, A. Szepes, O. Laczkovich, P. Szabó-Révész, K. Pintye-Hódi, I. Erős, T. Haasner, J. Ulrich: Use of melt solidification for the development of iron(II)sulfate-containing drop-formed particles, *BIWIC 2002-9th-International Workshop on Industrial Crystallization, 11-12. Sept., 2002, Halle, Germany*

VII. ***Pallagi E.***, Szabóné Révész P., J. Ulrich, Erős I.: Glicerin-származékok alkalmazása a vas(II)-szulfát olvadékból történő szemcseképzése során, *XII. Congressus Pharmaceuticus Hungaricus, Budapest, 2003. május 8-10.*

VIII. ***E. Pallagi***, P. Szabó-Révész, J. Ulrich, I. Erős: Use of glycerine derivatives in melt solidification for the development of iron(II) sulfate-containing particles, *BIWIC 2003-10th-International Workshop on Industrial Crystallization, 4-5. Szept., 2003, Rouen, France*

IX. ***E. Pallagi***, P. Szabó-Révész, J. Ulrich, I. Erős: New possibilities for the development of iron(II) sulfate-containing solid products with sustained drug release, *International Meeting on Pharmaceutics, Biopharmaceutics and Pharmaceutical Technology 2004, 15-18. March, 2004, Nürnberg, Germany*

X. B. Farkas, T. Gregor, K. Nagy, ***E. Pallagi***, P. Szabó-Révész, I. Erős: Spherical crystallization of iron(II) sulfate heptahydrate for development of solid dosage form, *BIWIC 2004-10th-International Workshop on Industrial Crystallization, 15-17. Szept., 2004, Gyeong-Ju, Korea*

Contents

1. Introduction

Modern pharmaceutical therapy increasingly demands the development of pharmaceutical products with controlled drug release and prolonged drug effect. The slow drug liberation from the product ensures better absorption and a steady drug level in the body, hereby the drug's therapeutical effect will be uniform.

The slow drug release has further advantages in certain cases. For example, iron(II) sulfate, one of the most commonly applied pharmacons in the therapy of anaemia, effects gastric mucosa irritation, which can be decreased remarkably by the slow liberation of iron. Another advantage of retard products is that they make one daily dose possible, and thus better patient compliance results.

The production of medicines with prolonged drug release is achievable with pharmaceutical technological methods. Pharmacists working in the field of pharmaceutical technology have expressed a definite need for new, simple, time- and cost-saving methods and also for new substances with suitable parameters for direct processing.

The so-called *melt technologies* are in the centre of interest again partly because of the new substances and methods, and partly because they usually make quick and simple manufacturing possible within a short time and at low costs. Another advantage is that they are environment-friendly and can be used for manufacturing solid products with controlled drug release.

Spherical crystallization, which ensures the production of basic material with appropriate parameters and properties, is also a field on which great interest is focussed nowadays. With the spherical crystallization process crystals with a round shape can be produced, and they make it possible to apply surface treatment (e.g. crystal coating) immediately or to perform direct tablet compression. The preliminary granulation of the substance is not necessary, which also contributes to its time- and cost-saving character. The powder rheological properties of round crystals are better, they can be filled into the capsules easily, thus giving the final product.

References to the author's own articles are made with bold numbers.

2. Aims

The aim of my PhD work was to produce solid dosage forms from *iron(II) sulfate* with the use of new pharmaceutical technological methods. The industrial processing of iron(II) sulfate and the production of solid dosage forms (tablets, capsules) with conventional methods are difficult, lengthy and expensive. Therefore new, time- and cost-saving methods are needed in iron processing, with special regard to slow and prolonged drug release from the product.

In my research work the following objectives were set:

⇒ The overview of the literature related to the subject;

⇒ The selection of the appropriates iron(II) sulfate hydrate form for melt technology with thermostability tests;

⇒ The study of crystallization from melt and from solution, and the processing of iron(II) sulfate using the melt solidification technology and the spherical crystallization process;

⇒ The investigation of the applicability and reproducibility of the above-mentioned technologies, the classification of the produced samples from aspects of pharmaceutical technology and biopharmacy.

3. Literature

3.1 Physiology of iron

Iron is an essential component for crucial cellular processes. It is necessary in the oxygen-transport as a component of haemoglobin and of enzymes in the respiration. Iron containing proteins are involved in the production of ATP and DNA-synthesis and other physiological processes [1, 2]. It is also essential for the regulation of cell growth and differentiation, e.g. in the central nervous system and in the growth of the brain. Consequently, the actual iron status influences the normal human physiology and the state of health [3].

An adult body contains approximately 3-5 g of iron and it needs on the average 1 mg iron per day. Healthy adults absorb about 10% to 15% of dietary iron [4], but individual absorption is influenced by several factors. In certain ages (infancy, adolescence) and states (menstruating- and pregnant women) iron requirements are

high [5, 6]. Iron absorbs mainly from the upper part of the small intestine [7]. Iron absorption is minimal from the stomach, but at acidic pH iron-ions dissolve and are reduced ($Fe^{3+} \rightarrow Fe^{2+}$). The new researches confirm that ferro (Fe^{2+}) ions are absorbed quickly and in a great quantity by passive diffusion [8, 9], and ferri (Fe^{3+}) ions assist in the physiological process of absorption and pass into the blood by active transport by means of mucosa-transferrin. Iron absorption is influenced decisively by the iron stores. The absorption increases when body stores are low and when iron stores are high, absorption decreases [7, 10-12]. If the iron intake is low and not enough to cover the requirement, a negative iron balance evolves. This negative balance results in iron deficiency and *iron deficiency anaemia* with typical symptoms [13-15].

3.2 Replacement of iron, iron therapy

In iron deficiency and anaemia it is necessary to take in iron. Among the medicines one can find iron containing tablets, capsules, syrups, effervescent tablets and injections [16, 17]. In the daily therapy usually iron salt containing medicines are administered orally. In cases of anaemia, tablets are generally used twice or three times a day (for a period of months) to fill up the iron stores [2]. The patients' compliance improves if only one medicine dose is necessary daily.

The typical side effects of iron therapy are gastrointestinal effects (e.g. nausea, diarrhoea or constipation, lack of appetite, epigastric ache, sometimes oversensitiveness), and the most common is gastric irritation as a result of the iron reaching the stomach suddenly in a high concentration [10, 16]. In modern therapy tablets with sustained release are preferred as they increase patient compliance and decrease the side effects.

Several iron salts are suitable for iron replacement (e.g. *ferrous succinate, ferrous lactate, ferrous fumerate, ferrous glycine sulfate, ferrous glutamate, ferrous gluconate, ferrous citrate, iron(III) hydroxide* etc.). The absorption of iron compounds is correlated with *iron(II) sulphate,* as it is a standard, its absorption is regarded as the 100% level [10]. At present several medicines available on the market contain iron(II) sulfate as their active agent.

3.3 Characteristics of iron(II) sulfate

It is difficult to work up iron(II) sulfate as a dosage form. The problems involved in the preparative technologies are the following:

⇒ *Oxidation*

Iron is oxidized easily ($Fe^{2+} \rightarrow Fe^{3+}$), which is provoked by humidity and heat. Upon the effect of oxidation the quantity of iron(II) and iron(III) ions changes in the preparation, which in turn influences the applicability, the effect and the safety of medicine.

⇒ *Corrosion*

One of the processing problems is that iron causes the attrition and corrosion of the machines within a short time. This is an extra cost of the production.

⇒ *Gastric irritation*

Gastric irritation can decrease considerably if the iron release from the product is slow with a uniform rate.

Iron(II) sulfate resides in crystal forms with 1-7 molecules of water. The water solubility of different hydrate forms is different and it varies with temperature (Fig. 1.).

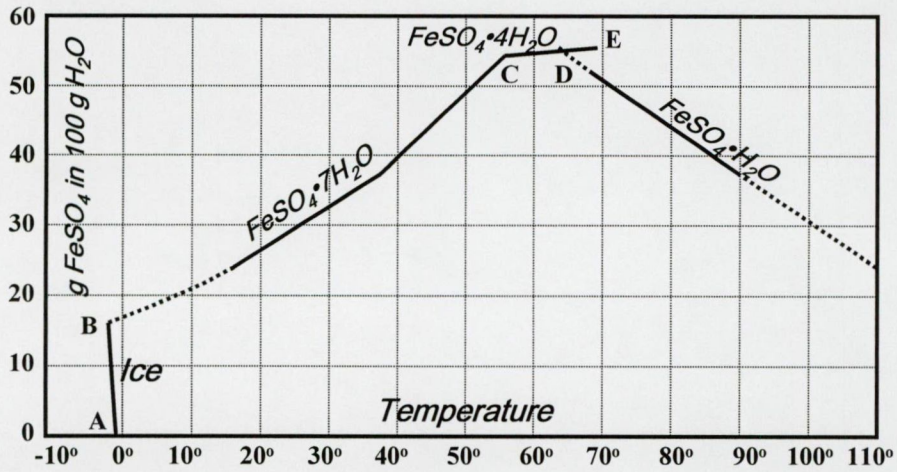

Fig. 1. The dissolution curve of iron(II) sulfate in water [18]

The iron(II) sulfate crystals soluted in water crystallize as *heptahydrate* from solution under adequate circumstances (e.g. temperature, saturation of solution etc.) [19-21].

By means of the crystallization of iron from the solution with the conventional crystallization process, the product's crystal form will ideally be *cubic*. Cubic crystals are shaped like cubes or boxes, the axis lengths and the axis angles are uniform ($a = b = c$, $\alpha = \beta = \gamma = 90°$). One of the atoms is located in the centre of the unit cell and the others are located at equal distances from it (*body-centered cubic (bcc) crystal system*) (Fig 2.) [22]. Moreover, iron(II) sulfate monoclinic crystals are also described in

literature. In the case of monoclinic crystals the three axes are unequal in length, two of them are at right angles, while the third is at an angle other than 90° ($a \neq b \neq c$, $\alpha = \beta = 90°$ and $\gamma \neq 90°$) [21, 23-27]. In the literature the axis lengths are as follows: a : b : c = 1.1828 : 1 : 1.5427 [18, 28-30], while the iron(II) sulfate heptahydrate available on the market is heterodisperse, with variable crystal shapes and sizes.

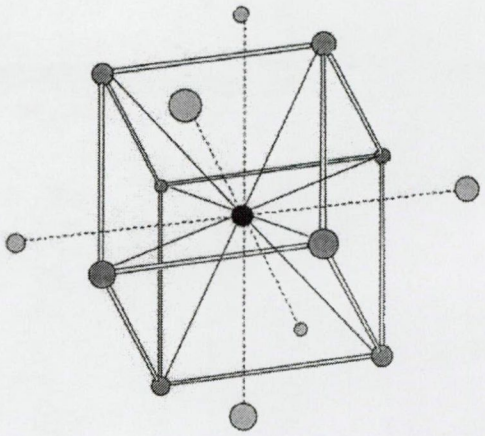

Fig. 2. The structure of a regular bcc-crystal

3.4 In general about crystallization

Crystallization is one of the oldest and most important processes, used in the food, pharmaceutical and chemical industries. It is used principally for purification and separation. Depending on the starting material, the crystallization process can take place *from solution* and *from melt*, but it is difficult to separate the two areas technically.

3.4.1 Crystallization from melts

3.4.1.1 Conventional crystallization from melts

Nowadays melt crystallization is used mainly in the preparation of raw materials [31], but it can also be applied in pharmaceutical technology. It is used for separation and purification [32-34] based on the various melting points of components. It is well applicable in the production of organic substances with high purity, for isomer separation, seawater desalination etc. [35]. From the energetical aspect melt crystallization is more advantageous than other separation techniques because it takes place at a lower temperature, so the phase transition enthalpy is lower, which is also favourable for heat-sensitive materials [36].

Classically melt crystallization means the melting of a material or material mixture and its solidification upon the effect of cooling. Only those materials can be crystallized from the melt which can be melted without decomposition and can be heated above the melting temperature in a melted state [37]. We can distinguish solid

layer and suspension melt crystallization [38]. Solid layer crystallization is based on the formation of a crystal layer on a cooled surface, and solid-liquid separation is also realized during the process. In suspension crystallization the solid product is present as crystals, which are freely suspended in the melt. Supersaturation is generated by the cooling of the melt. Both the layer- and suspension-based processes can be carried out with continuous or fractional, and static or dynamic procedure [39].

The kinetics of melt crystallization is simpler than the kinetics of crystallization from solution. The phase of nucleation and phase of crystal growth can be distinguished in the process of crystallization. Temperature transport plays an important role in the process, and there is primary heterogeneous nucleation indicated by an artificial centre [36]. In the melt suspension crystals can grow freely, but in the layer the surface and the neighbouring crystals limit the crystal growth. Hence it is better to use the term layer growth instead of crystal growth [40].

3.4.1.2 Melt technologies

Several melt technologies are used such as melt-granulation [41], melt-extrusion [42-45], technologies based on dropping or spraying of the melt [46, 47]. These are applied in pharmaceutics to give shape, to increase the solubility or bioavailability, to modify the release of the active agent or to work up materials which cannot be processed by traditional methods. It is also applicable to prepare products with sustained drug release [48, 49]. In these cases usually the auxiliary material is melted and not the drug. In the melt technology auxiliary materials such as polyethylene-glycols [50, 51], waxes [52, 53], stearine [54], fats, fatty acids, fatty alcohols, glycerides [55, 56] and glycerine derivatives [57] can be used. In these cases the mechanism of drug release from the products is erosion and diffusion [58, 59].

A new and modern method in the field of pharmaceutical technology is the melt solidification technique from drop (*special hot melt technology*). It is a melt crystallization technology, which means the solidification from melt in drop form [60]. It is used mostly for the purpose of giving shape, and it is well applicable in the preparation of raw materials with varied shape and in great quantities if the uniform shape, surface and size are basic requirements [61-63]. The chemical industrial machine and the different feeders are shown in Figure 3. and Figure 4.

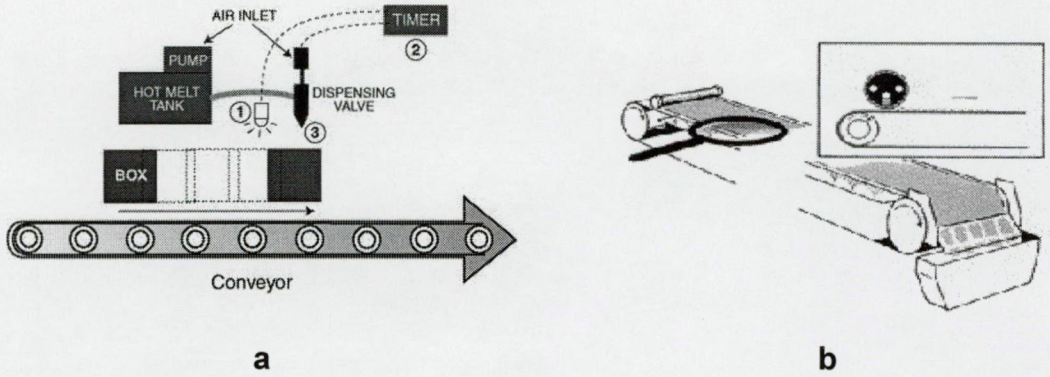

Fig. 3. The principle of operation (**a**) and the industrial machine (**b**) for the melt solidification in drop [64]

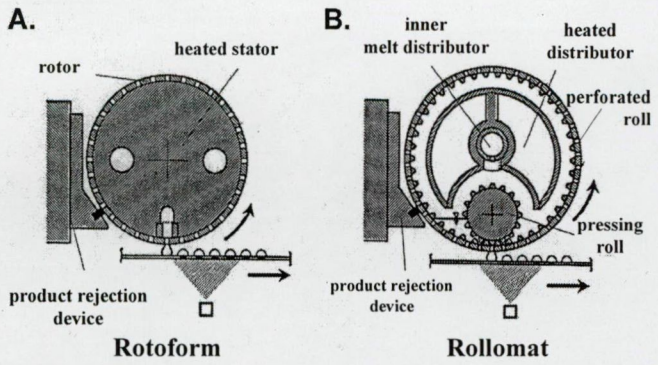

Fig. 4. Different feeders to the melt solidification technology [65]

3.4.1.3 Determination of surface free energy for the melt solidification technology

The product shape is influenced by the surface free energy of the cooling surface in the melt solidification technology. The surface free energy can be calculated from the contact angles between the surface and test liquids [66-70]. Contact angles can be determined with *Drop Shape Analysers* [71]. There are many different theories for the calculation of the surface free energy on the basis of contact angles with such an analyser [72-77].

The theory of *Owens and Wendt* is based on the different wetting properties of the liquid on different surfaces (Fig.5.). On the other hand, the contact angles of different liquids on the same surface are different.

water on glass water on teflon water on steel

Fig. 5. Contact angles of water on different surfaces

This is the *wetting* phenomenon, which can be explained by the interaction between interfaces, by the surface free energy, and it is also influenced by adsorption and the liquid properties [78-**80**, 81]. The most important parameter of wetting is the contact angle (Θ = theta) (Fig. 6.).

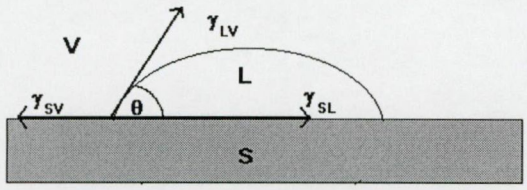

Fig. 6. Contact angle (Θ) between solid surface and liquid

where: γ_{SV} = interfacial tension between solid surface and vapour, γ_{SL} = interfacial tension between solid surface and liquid, γ_{LV} = interfacial tension between liquid and vapour

The thermodynamics of the contact angle is described by the *Young equation* (1805) [82]. The behaviour of the liquid drop is determined by the interfacial tensions arising among the three interfaces (γ or σ), and according to the Young equation equilibrium arises when the vector sum of the surface forces is zero.

$$\cos\theta = \frac{\gamma_{sv} - \gamma_{sl}}{\gamma_{lv}}$$

The Young equation

Theoretical relationships by Owens et al. [74]

The interfacial tension of a liquid (γ_l) results from the polar (γ_l^p) and disperse (γ_l^d) component of interfacial tension (1). The same applies to the interfacial tension of a solid phase (γ_s) (2).

$$\gamma_l = \gamma_l^d + \gamma_l^p \qquad \gamma_s = \gamma_s^d + \gamma_s^p \qquad (1), (2)$$

The interfacial tension between the solid surface and the liquid drop can be calculated with (3), (4):

$$\gamma_{sl} = \gamma_s + \gamma_l - 2\left(\sqrt{\gamma_s^d \cdot \gamma_l^d} + \sqrt{\gamma_s^p \cdot \gamma_l^p}\right) \qquad (3)$$

$$\cos\Theta = f\left(\gamma_s, \gamma_s^d, \gamma_l, \gamma_l^d\right) \qquad (4)$$

If the contact angles and the γ_l^p and γ_l^d (from data base) of test fluids are known, x-y pairs can be composed according to the above equations (5), (6):

$$\sqrt{\frac{\gamma_l - \gamma_l^d}{\gamma_l^d}} = \sqrt{\frac{\gamma_l^p}{\gamma_l^d}} = x \qquad \frac{1+\cos\theta}{2} \cdot \frac{\gamma_l}{\sqrt{\gamma_l^d}} = y \qquad (5), (6)$$

It leads to the $y = mx + b$ line equation, and from this the surface free energy can be calculated (7), (8):

$$\gamma_s^p = m^2 \text{ and } \gamma_s^d = b^2 \tag{7}$$

$$\downarrow\downarrow$$

$$\gamma_s = \gamma_s^d + \gamma_s^p \tag{8}$$

3.4.2 Crystallization from solution

The crystallization from solution takes place in the supersaturated solutions [83, 84]. Supersaturation can be achieved both in physical and chemical ways, e.g. heating or cooling of the solution or the salting-out method. It is very important to know the solubility diagram of the material (Fig. 7.). The main characteristics of this diagram are the metastable and the instable zones. In the instable zone the spontaneous formation of crystal nucleus occurs, while the growth of the crystals is observable in the metastable zone. The crystallization process can be governed in this zone and it can usually be determined experimentally [85, 86].

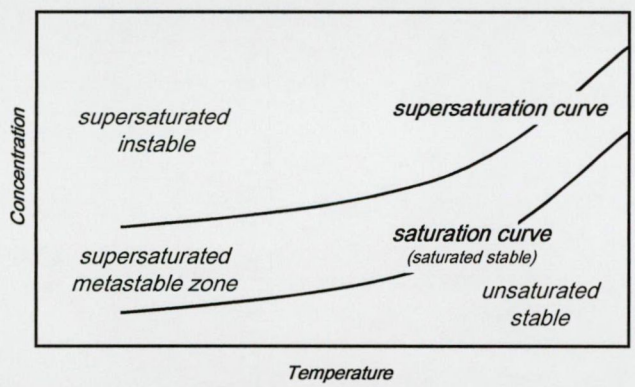

Fig. 7. Solubility diagram

Nucleation and crystal growth are the two important phases of crystallization. The diagram of nucleation is presented in Figure 8.

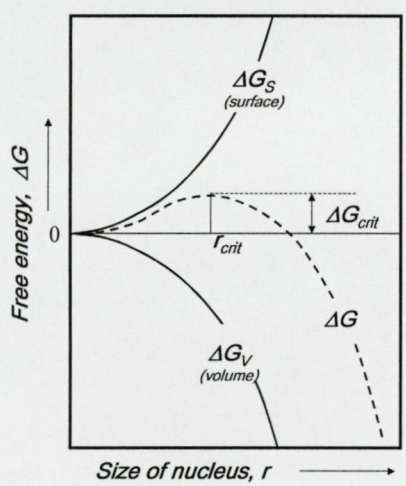

Fig. 8. The diagram of nucleation

The nucleation rate (J) is influenced by the change of the surface free energy of the particle (ΔG) [87] and it can be expressed by:

$$J = \exp(-\Delta G/kT)$$

where

J = nucleation rate, ΔG = free energy between a small particle of solid solute and the solute in solution, k = rate constant, T = temperature.

The particle size belonging to the maximum level of the ΔG curve is the critical particle size, where either crystal formation is started or the particle will be resoluble [88].

The phase of crystal growth means the formation of a regular lattice from molecules. The rate of crystal growth can be described by:

$$R = (1/A_T)\cdot(dW/dt) = k_G\cdot\Delta c^g$$

where

R= overall growth rate based on mass deposition, A_T= total crystal surface area, W= mass of crystals, t= time, k_G= growth rate constant, Δc^g= concentration of crystal [89].

With adequate parameters (e.g. cooling rate, rotation speed of mixer, solvent, seed crystal etc.) it is possible to change the morphological properties and the crystal habit during the crystallization process from solution, hereby spherical crystals can also be produced with this method. This is the so-called *non-typical spherical crystallization* process. The alteration of the morphological properties results in better flowability and compressibility, and it also makes the materials suitable for direct compression. If the traditional crystallization processes are not suitable for the preparation of spherical agglomerates, the *typical spherical crystallization process* can also be used. This technique was defined first by Kawashima [89]. The *typical spherical crystallization process* employs three solvents: one is the substance dissolution medium, another is the medium which partially dissolves the substance and the third is the wetting solvent for the substance [90]. In the three-solvent system the dissolved drug material is carried in emulsion drops. Later the drops become oversaturated with respect to the drug material and in situ seed formation starts followed by crystal formation. Therefore the emulsion drop-size determines the size of crystal agglomerates. Many drugs have been successfully transformed into spherical agglomerates with this technology [91-97].

3.5 Prolonged drug effect, the pharmaceutical-technological possibilities of prolongation

From the conventional peroral dosage forms the active agent is liberated quickly, through absorption the plasma drug level increases continuously and, having reached the maximum concentration (C_{max}), it decreases until complete elimination. In conventional therapy repeated administration is necessary to maintain the required drug concentration in blood [98]. If the dose size and the frequency of administration are chosen correctly, the therapeutic "steady state" levels of drug can be achieved and maintained. However, there are a number of potential limitations associated with repetitive administration of conventional dosage forms [99, 100].

Nowadays pharmaceutical technological researches tend to develop dosage forms with sustained release [**101**, 102]. These sustained release preparations are designed to release the drug contained therein at a continuous and more controlled rate for a longer period of time [103-105]. Consequently, peroral administration of a "single dose" of a sustained release product increases the duration of therapeutic action and the therapeutic effect of the drug contained therein beyond the level achieved normally with a single dose of the corresponding non-sustained conventional counterpart.

The in vivo effect of a drug is mostly demonstrated by the plasma-concentration-time curve [98]. The parameters calculated from the curve (k_a, k_e, $t_{½abs}$, $t_{½\,elim}$, AUC, t_{max}, C_{max}, MAT, MRT, BH_{abs}, BH_{rel}) characterize the drug effect [106].

The most important kinetic parameter for a sustained release preparation is the liberation at a constant rate, which ensures the constant plasma drug level in a longer period of time [107]. This is called zero order kinetics [49, 51]. According to zero order kinetics, the rate of release is constant and independent of the amount of the maintenance dose remaining in the dosage form. Ideally, the preparation consists of two portions, the first provides the initial dose which releases rapidly, and the second is the maintenance or sustained dose with slow drug liberation [100].

There are several formulation methods for achieving sustained drug release. Applicable technologies include classical coating, embedding of drug in a wax, fat or plastic material, microencapsulation, chemical binding to ion-exchange resins and incorporation in an osmotic pump [49, 51, 108, 109]. These processes can be used in combination as well.

4. Materials and methods

4.1 Materials

Iron(II) sulfate monohydrate (Ph. Eur. 3., Merck Eurolab GmbH, Darmstadt, Germany) was used as the active agent for the production of solid particles with special hot melt technology. The particle size was 44-104 μm. The auxiliary materials (bed materials) were *white wax* (Cera alba, melting range: 62-66 °C, Ph. Hg. VII., Hungaropharma, Budapest, Hungary,), *stearin* (Stearinum, melting range: 54-67 °C, Ph. Hg. VII., Hungaropharma, Budapest, Hungary) which is a mixture of stearic acid and palmitic acid, *Compritol ATO 888®* (glyceryl behenate, Ph. Eur. 3., Gattefossé, France, melting range: 69-74 °C) and *Precirol ATO 5®* (glyceryl palmitostearate, Ph. Eur. 3., Gattefossé, France, melting range: 53-57 °C).

The basic material in spherical crystallization was iron(II) sulfate heptahydrate available on the market (Ph. Hg. VII., Hungaropharma, Budapest, Hungary) with 10 μm –2 mm particle size. Stearin (Stearinum, Ph. Hg. VII., Hungaropharma, Budapest, Hungary) was used as the coating material during the coating process.

4.2 Methods

4.2.1 Preformulation studies

4.2.1.1 Reactions kinetic investigations

The aim of the reactions kinetic investigations was to select the iron-compound that is applicable in melt technology. Samples of iron(II) sulfate monohydrate and heptahydrate were stored in a furnace at 120 and 160 °C for 2 hours. Samples were taken after 0.5, 1 and 2 hours. The iron(II)-concentration of the samples was measured by an analytical method based on a colour reaction. Fe^{2+}-ions and 2,2'-bipyridil compose a red and water-soluble complex which can quantitatively be measured spectrophotometrically at 522 nm [110-112] and the activation energy can be calculated [113-115]. The activation energy is the amount of energy required for a reaction, the difference in energy between the initial state and activated state.

4.2.1.2 Thermostability test

The thermostability test was carried out in accordance with the guidelines of ICH-International Conference on Harmonization, signed as Q1A [116]. The changing

of the Fe^{2+} content was measured in time by means of the already mentioned colour reaction. The Fe^{3+}content of the samples was calculated in such a way that the actually measured Fe^{2+}content was subtracted from the total iron content.

4.2.2 Product development

4.2.2.1 The method of melt solidification in drops (special hot melt technology)

Preformulation studies for the special hot melt technology

The surface free energies of different cooling surfaces (enamel, steel and teflon surfaces) were measured. 3 test fluids such as distilled water, diiodomethane and glycerine were used for all the measurements, with known polar and disperse parts of their interfacial tensions. The contact angles were measured for all the surface materials with a Krüss Drop Shape Analyser (DSA, G10, Krüss, Hamburg) and their surface free energies were calculated according to the theory of Owens et al. [74]. 3 parallel examinations were carried out in each case.

The contact angle of a solid particle can be measured with the Drop Shape Analyser. The contact angle of an ideal spherical particle is 180°. Solid particles were produced with the special hot melt technology at different temperatures. The contact angles of the produced particles were measured. The melt of stearine and steel surface were used in the course of the investigations.

Product development with special hot melt technology

The essence of this method is the drop forming of the melted material with laboratory equipment and the solidification of drops on the cooling surface at a definite surface temperature [38, 117, 118]. After the determination of the process parameters (temperature, the material of cooling surface, drop-size etc.), particles with various shapes can be produced with this method [64].

The method of melt solidification is a special hot melt technology, practically a modified dropping process. The advantage of this technology is that shape formation (spherical particles) and drug release regulation are realized in one production step [**119**]. The other advantage is that it is a solvent-free, consequently an environment-friendly process. The laboratory equipment developed by Bülau and Ulrich was used for the production [117]. The most important parts of this equipment are the heated pipette and the pastillation cell with cooled surface (Fig. 9.).

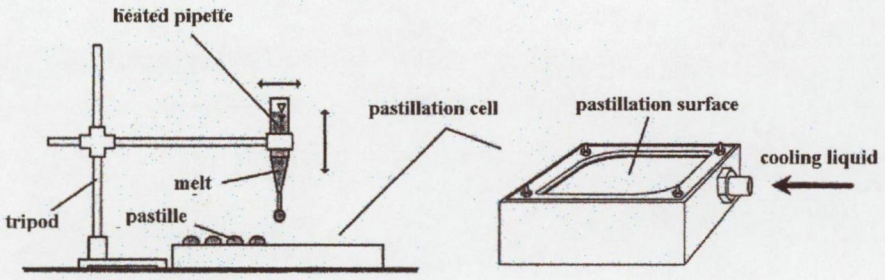

Fig. 9. Special laboratory equipment for melt solidification [117]

The process parameters such as the temperature of the melt, the temperature and the material of the cooled surface, the size of the drops and the distance between the pipette and the cooled surface could be varied. After the determination of process parameters in preformulation studies, the production of spherical solid particles is fast and simple [**120**]. The geometrical properties of the particles are influenced by the material and the surface free energy of the cooling surface as well as by the temperature of the surface and the melt.

The process of this melt solidification technology is the following: iron(II) sulfate is suspended and homogenized in the molten bed materials. This suspension is dense with high viscosity and is prepared in a double-walled glass connected to a thermostate. This suspension is mixed at 50 rpm. The preheated melt (suspension) is dropped onto a cooled surface at adequate temperatures by means of a heated pipette (pipette diameter: 1.2 mm). The dropping height of the melt is 6 mm. After dropping the suspension solidifies without any deformation effect of cooling, thus the procedure results in round solid particles (Fig. 10.).

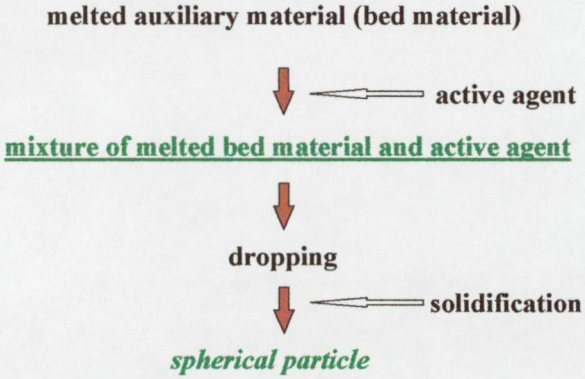

Fig. 10. The scheme of the special hot melt technology

4.2.2.2 Spherical crystallization

Preformulation studies for spherical crystallization

The aim of the preformulation studies was to examine the effect of the crystallization process parameters on the produced samples with a view to produce iron(II) sulfate heptahydrate spherical crystals. We used the non typical spherical crystallization process from solution. A SCHMIZO duplicate reactor crystallizer with 0.5 l volume was used equipped with a mixer, the mixing speed of which could be regulated. The crystallization process can be realized according to different cooling programs with a thermostat connected to the set. The concentration of the saturated solution was constant (135 g $FeSO_4 \cdot 7\ H_2O$/100 g water). During the preformulation studies the starting temperature, the cooling rate, the cooling mode, the speed of the mixer and the solvent were varied. The necessity of the seeding crystal was also studied. The samples were produced at laboratory scale.

Melt-coating of spherical crystals

The scale-up process of the lab-sample the parameters of which were optimal on the basis of preformulation study was performed, and 100.0 g of the iron(II) sulfate heptahydrate crystals (Fe/12) with a diameter of 0.5-1 mm was coated. This was carried out in a rotating steel pan, with stearin used as the coating material. The carrier liquid of the melted stearin was 95% alcohol. An air spray technique was used for the atomisation of the liquid. The process parameters were as follows: nozzle diameter: 0.8 mm, atomisation air pressure 0.1 bar, flow rate of coating liquid: 5 ml/min, coating liquid temperature: 60 °C, drying air temperature: 20 ± 2 °C and pan rotation speed: 25 rpm.

4.2.3 Measuring methods

• *Stereo microscopic study*

The habits of the particles were studied with a Zeiss stereo microscope (Zeiss KL 1500 LCD, Jena, Germany).

• *Electron microscopic study*

The properties of the formulations (surface and cross-section) were observed by scanning electron microscopy (Hitachi 2400S Hitachi Scientific Instrument Ltd., Tokyo, Japan). A Polaron sputter coating apparatus (Polaron Equipment Ltd.,

Greenhill, UK) was applied to induce electric conductivity on the surface of the sample. The air pressure was 1.3-13 mPa.

• *Particle size analysis*

The particle size analysis of samples produced with special hot melt technology was performed with a screwmicrometer (Mitutoyo, Tokyo, Japan). The mean diameter was calculated from the linear size of 100 particles, with accuracy to three decimals.

The particle size of the particles produced by the crystallization process was measured by sieve analysis (DIN ISO 3310, Retsch GmbH & Co., Haan, Germany).

• *Determination of roundness*

To determine the roundness of the particles produced with the crystallization process, an image analyzer (Laborlux light microscope, Quantiment 500MC image analyzer – LEICA Cambridge Ltd., Anglia) was used. Its software makes it possible to measure the length and the diameter of the particles and also to calculate the roundness according to the following relationship [121]:

$$\text{roundness} = \text{perimeter}^2/4\Pi \cdot \text{surface area} \cdot 1{,}064$$

The value of 1.064 is the correction factor of the perimeter. If the roundness value is about 1, the investigated particle's shape is approximately round.

• *X-ray powder diffraction (XRPD)*

X-ray powder diffraction profiles were taken with an X-ray diffractometer (Philips PW 1050/70 PW 1710). The measurement conditions were as follows: radiation source: CuK_α , scan speed: 0.035 (2θ), step size: 0.035 (2θ), time per step: 1.0 s.

• *Thermoanalytical tests*

In order to observe the physical and chemical changes arising upon the effect of heating, thermoanalytical investigations (TG-, DTG-test) were performed with a MOM apparatus (MOM, Budapest, Hungary). The test parameters were the following: mean sample weight: 50 mg, heating rate: 5 °C/min. The studies were performed in air atmosphere.

• *Mass measurement*

This measurement was performed with an analytical balance (Sartorius H 110) with four-decimal accuracy. The mean particle mass was calculated after the measurement of 100 particles in accordance with the Ph. Hg. VII.

• *Determination of the total iron content*

The total iron content of the investigated samples was determined by atomic absorption method. The samples were submitted to a burning process and the residue was dissolved in the mixture of diluted hydrochloric acid and sulphuric acid. The solution was diluted into the concentration range where it could be measured. Measurements were carried out with a Perkin Elmer 4100 atomic absorption spectrometer (Bodenseewerk Perkin Elmer GmbH, Überlingen, Germany) at 248.3 nm in air-acetylene gas. The iron content of each particle is given with respect to iron(II) sulfate monohydrate.

• *Determination of iron(III)-content*

Fe^{2+}-ions form a colourful complex with 2,2'-bipyridil in an acidic medium, the colour intensity of which can be measured spectrophotometrically (Spectronic Unicam, Helios Alpha, Cambridge) at 522 nm. The Fe^{3+} content was determined by subtracting the actually measured Fe^{2+} content from the total iron content of the sample.

• *Measuring of flow time and bulk density*

The volume of 100 ml from each sample was investigated to determine flow time and bulk density (g/100 ml) with the ASTM-D (USA-standard) apparatus official in the Ph. Hg. VII. 6 parallel measurements were performed for each sample.

• *In vitro drug dissolution study*

Dissolution studies were performed with a Pharma Test PTW 2 apparatus (Pharma Test GmbH, Hainburg, Germany) paddle method, under sink conditions. The medium was 900 ml of artificial gastric fluid (pH = 1.2 ± 0.1) with a temperature of 37 ± 0.5 °C. The rotation speed was 100 rpm. Samples of 5 ml were extracted at regular time intervals. The sample-times were 0.5, 1, 2, 3, 4, 5, 6 h and 0.5, 1, 2, 3, 4 h. The samples were analysed with a Perkin Elmer 4100 atomic absorption spectrometer (Bodenseewerk Perkin Elmer GmbH, Überlingen, Germany) under the following conditions: flame-atomizing, wavelength 248.3 nm, slit width 0.7 nm, air-acetylene gas mixture (air: 0.8 L/min, acetylene: 3.5 L/min), and read time 5 s.

• *In vivo study*

New Zealand white rabbits (mean body weight 2632 ± 155 g), 6 animals in each group, were treated orally with the particles (dosage: 20 mg iron(II) sulfate/kg). The particles were introduced directly into the stomach via a catheter and were

washed in with 30 ml of water. The control animals were treated with an equivalent dose of iron(II) sulfate in aqueous solution (0.5% w/v). Blood samples were collected from the marginal ear veins 12 or 14 times, at 0, 0.5, 1, 1.5, 2, 3, 4, 5, 6, 7, 8 and 10 h, with two additional samples at 0.25 and 0.75 h for the aqueous solution. Heparin was used as anticoagulant. Samples were stored at 5 °C until analysis.

Afterwards, the animals were anaesthetized with iv. pentobarbital, the mucous membranes of the stomach and ileum were examined and the macroscopic changes were evaluated.

Animal investigations were carried out with the approval of the Ethical Committee for Animal Research, University of Szeged (registration number: I-74-7/2002).

Evaluation of the active agent:

Iron(II) concentrations in plasma samples were measured with the aid of a Ferrozin kit (Diagnostikum Rt, Budapest, Hungary). At pH = 4.8, Fe^{3+} dissociates from transferrin and is reduced to Fe^{2+} by the ascorbic acid incorporated in the kit. This Fe^{2+} forms a red complex with ferrozin. Its absorbance at 560 nm is directly proportional to the Fe^{2+} concentration. The test is linear up to a Fe^{2+} concentration of 179 μmol/L.

For the analysis, 200 μl of plasma or standard solution was used. The plasma Fe^{2+} concentrations were measured against a reagent blank. The physiological Fe^{2+} concentration was determined on blood samples taken at 0 h, just before the treatment. This value was subtracted from the Fe^{2+} concentrations measured after the treatment.

Pharmacokinetic evaluation

Computerized data processing was carried out with MEDUSA 1.8. Curves were fitted to the concentration values within each group and pharmacokinetic analysis was performed in accordance with the one-compartment open pharmacokinetic model.

The plasma concentration curve was plotted and the main pharmacokinetic parameters were determined: the absorption half-life ($t_{1/2abs}$), the elimination half-life ($t_{1/2elim}$), the mean residence time (MRT), the time to peak (t_{max}) and the peak concentration (C_{max}). The area under the curve (AUC_{∞}) needed for the estimation of the bioavailability was also calculated [122].

• *Statistical calculations*

The kinetic calculations (rate constant, correlation coefficient, slopes, intercepts) of the in vitro dissolution tests were performed with Excel, with a confidence level of 95%. The statistical evaluation of the kinetic parameters of the in vivo results was performed by SPSS ANOVA one-way statistical analysis.

5. Results

5.1 Result of thermostability assays

The heat resistance of iron(II) sulfate monohydrate and heptahydrate available on the market was investigated because of the inclination of iron-compounds to oxidation. The aim of our research was to establish which iron hydrate form tolerates the heat better and is suitable for the special hot melt technology. In order to obtain the desired results, reaction kinetic and thermostability tests had to be performed [**123**]. The samples were heated and the Fe^{2+} content decrease was detected. On the basis of this change, the order of reaction was defined and the activation energy was calculated with the Arrhenius-equation. The results of reaction kinetic tests are shown in the Table 1.

Table 1. Results of reaction kinetic test

	Equation of decomposition	Order of decomposition	Activation energy
Iron(II) sulfate heptahydrate	120 °C: $y = 323.3 \cdot e^{-0.5095x}$, $R^2 = 0.997$	***First order***	21299.8 J/mol
	160 °C: $y = 301.28 \cdot e^{-0.9302x}$, $R^2 = 0.9895$		
Iron(II) sulfate monohydrate	120 °C: $y = -5.7994x + 326.94$, $R^2 = 0.8983$	***Zero order***	4942.2 J/mol
	160 °C: $y = -6.668x + 326.63$, $R^2 = 0.9003$		

The decomposition of the heptahydrate form can be described with an exponential equation, which means that decomposition is carried out according to first order kinetics, namely the rate of decomposition depend on the amount of the starting material. The decomposition of iron(II) sulfate monohydrate can be described with a linear equation, so this is a zero order kinetic reaction. The reaction rate is constant in time.

The difference between the values of the activation energies was significant. The activation energy of iron(II) sulfate heptahydrate is greater with one order, so the same increase in temperature results in oxidation happening at a considerably greater rate while iron(II) sulfate monohydrate can tolerate the increase of temperature to a greater extent.

Therefore the thermostability test of iron(II) sulfate monohydrate was also performed according to the guidelines of ICH (Table 2.) Table 3. shows the parameters of investigation and the detected Fe^{3+} content of samples.

Table 2. Parameters of the thermostability test according to ICH Q1A protocol

	Long term testing	Accelerated testing
Temperature (°C)	25 ± 2	40 ± 2
Relative humidity (%)	60 ± 5	75 ± 5
Time (month)	12	6

Table 3. Parameters and results of the thermostability test

Samples	Container	Temperature (°C)	Relative humidity (%)	Fe^{3+} content of samples* (%)
1	glass, opened	20-23	40-45	2.45
2	plastic, guaranteed snap	20-23	40-45	1.78
3	glass, opened	25	60	3.02
4	plastic, guaranteed snap	25	60	2.50
5	glass, opened	40	75	2.38
6	plastic, guaranteed snap	40	75	1.84

* at the end of the test

The results show that iron(II) sulfate monohydrate is not oxidized to a great extent under the above-mentioned conditions. The greatest change in the Fe^{3+} content was about 3%.

It can be established that oxidation is slow in iron(II) sulfate monohydrate stored at a high temperature, high relative humidity and for a long period of time. This confirms the results of the reaction kinetic test.

The results of the investigations of reaction kinetics and thermostability revealed that the formulation of a solid dosage form of iron(II) sulfate hydrate forms can be realized in the way shown in Figure 11., and iron(II) sulfate monohydrate is suitable for the purpose of special hot melt technology.

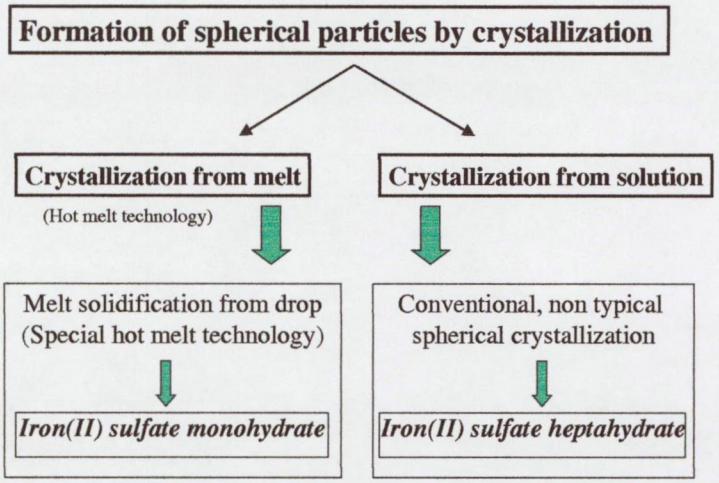

Fig. 11. Processing possibility of iron(II) hydrate forms (monohydrate and heptahydrate)

5.2 Results 1-The results of investigations of samples developed by melt solidification technology

Pre-formulation studies with an aim to prepare samples using the melt solidification technology

In the melt solidification technology (special hot melt technology) an important parameter which influences the shape of the produced sample is the surface free energy of the cooling surface. The surface free energy determines the contact angle between the drop and the cooling plate and if the melt-drop keeps its drop shape or flows on the surface during the solidification time. Three different surfaces such as enamel, steel and teflon were tested and the surface free energies calculated [**120, 124**] (Table 4.).

Table 4. The surface free energies of the tested surfaces

Surface material	Line equation	γ_s^p (mN/m)	γ_s^d (mN/m)	Surface free energy (mN/m)
Enamel	y = 4.958x + 5.1569	24.58	26.63	**51.21**
Steel	y = 2.2003x + 4.9999	4.84	24.90	**29.73**
Teflon	y = 2.0393x + 3.8067	4.18	14.44	**18.61**

Melt solidification technology requires a surface with moderate surface free energy. In the case of high surface free energy the melt drop may become deformed during solidification, and on a surface with low surface free energy the drop may flow before solidification as a round particle. Consequently, our choice fell on steel surface in processing iron with special hot melt technology.

The shape and structure of the resulting particles depend strongly on the temperature of the melt during drop formation and on the temperature of the solidification surface. We tested the effect of temperatures on the resulting particles in preformulation studies. First the melt of stearine with temperatures of 55, 60, 65, 70 and 80 °C was dropped onto a steel surface, the temperature of which was constantly 6 °C. In the second part the temperature of melted stearine was constant (60 °C) and the temperature of the cooled surface was varied (2, 6, 10, 20, 30 and 40 °C). The contact angle of the resulting solid particles was measured (Fig. 12-13.).

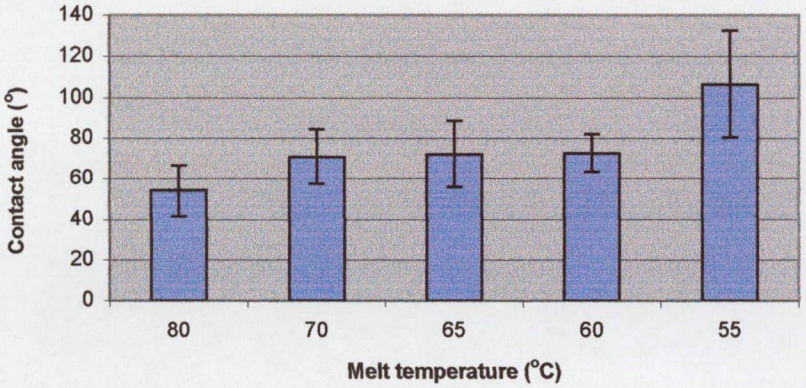

Fig. 12. Effect of the melt temperature on the contact angles of the particles using the melt of stearin (the surface temperature was constant at 6 °C)

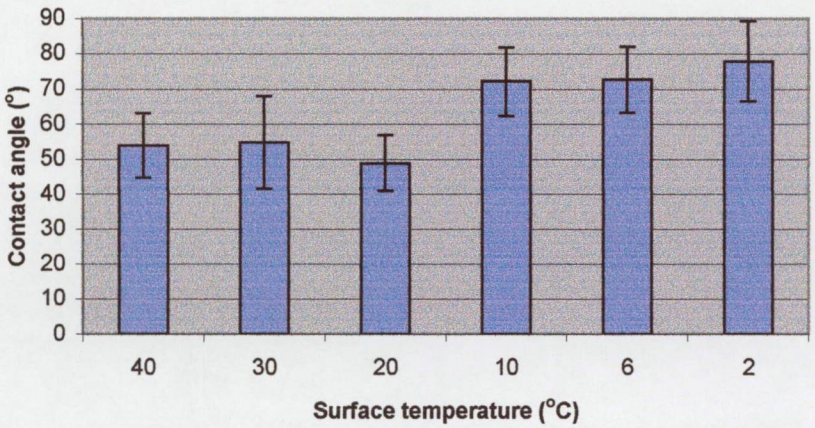

Fig. 13. Effect of the surface temperature on the contact angles of the particles using the melt of stearin (the melt temperature was constant at 60 °C)

The figures show that the contact angle of the melt increases with the decrease of the melt temperature. The effect of the melt temperature is more remarkable than the effect of the surface temperature. If the melt temperature is close to the solidification temperature, a sudden increase can be observed in the theta values. The shape of the product is then mostly spherical. Such a sudden change cannot be observed in the case of the surface temperature. The decrease in the surface temperature influences the contact angle only with a few degrees but it does not lead

to a considerable change in the shape of the product. Thus it can be established that during the special hot melt technology the melt temperature has a greater effect on product shape than the surface temperature where the melt solidifies. And if the melt temperature is near the solidification temperature, the solidification time can be decreased considerably and the occasional drop deformation can be prevented.

Table 5. shows the results of the same investigation of other auxiliary materials (white wax, mixture of stearin and white wax, Compritol ATO 888® and Precirol ATO 5®) and of stearin. The results are similar, namely the lower melt temperature of the tested auxiliary materials resulted in a particle with greater contact angle. After preliminary studies 5 samples were produced with special hot melt technology (Table 6).

Table 5. Drop forming properties of auxiliary materials and the contact angles of produced samples as shape characteristics

	Stearin	**White wax**	**Stearin and white wax (1:1)**	**Compritol ATO 888®**	**Precirol ATO 5®**
Melting range (°C)	**54-67**	**62-66**	**-**	**69-74**	**53-57**
$T_{melt}/T_{surface}$	**Contact angles of products (Θ/°)**				
53.4/10.6	106.62	-		-	158.24
57.9/10.6	72.64	-	152.49	-	157.76
62.4/10.6	72.24	145.34	142.81	-	158.64
66.8/10.6	71.00	136.83	132.93	144.29	156.70
71.4/10.6	-	99.50	126.28	139.27	-
76.0/10.6	54.26	99.64	114.28	144.12	158.96
80.8/10.6	-	99.44	103.96	149.52	-
76.0/20.2	-	-		*158.06*	-
80.8/20.2	-	-		*156.54*	-

Table 6. The composition of samples and the process

Product	**Auxiliary material**		**Amount of auxiliary material (%)**	**Amount of active agent (%)**	**$T_{surface}$ (°C)**	**T_{melt} (°C)**	**Viscosity (Pa·s)**
Sample 1	Natural	Stearin	50	50	10.6	57.9	0.401 ± 0.243
Sample 2		White wax	50	50	10.6	66.8	0.384 ± 0.008
Sample 3		Stearin-white wax	25-25	50	10.6	66.8	0.850 ± 0.0258
Sample 4	Semisynthetic	Compritol 888 ATO®	50	50	20.2	76.0	2.946 ± 1.673
Sample 5		Precirol ATO 5®	50	50	10.6	62.4	2.09 ± 0.842

Using the process parameters presented in Table 6., almost round particles can be produced and the contact angle of particles can be measured with the help of a Drop Shape Analyser. A picture of the produced particle made with a CCD camera connected to the DSA equipment can be seen in Figure 14.

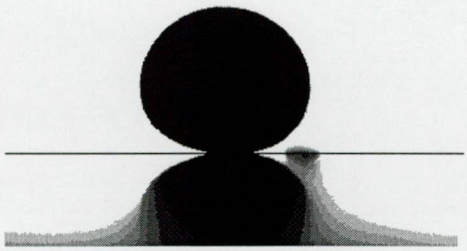

Fig. 14. Picture of solid particle produced by special hot melt technology,Sample 2, Theta: 174 ± 0.1°

5.2.1 Application of natural bed materials (stearine and white wax) in melt technology

Pharmaceutical technological evaluation of samples

For the development of the iron(II) sulfate-containing lipophilic matrices, we used a special hot-melt technology (melt solidification in drops) which provides solid spherical particles. Natural bed materials such as stearine and white wax were used. The pharmaceutical technological parameters of the samples 1-3 are shown in Table 7. The mass and the size of samples are both uniform. The mean mass is around 10 mg and the mean sample diameter is about 2 mm. The low values of the standard deviations confirm that the production of the samples is well reproducible. The cause of the similar parameters is the similar drop forming properties and viscosity of the melt of bed materials.

The iron(II) sulfate monohydrate content of particles is between 6 and 7 mg. The low standard deviations demonstrate that sample production with this technology is reproducible with respect to homogeneous drug content. The iron present in the product is not oxidized considerably during the process. The Fe^{3+}-content in the product is only 0.02-0.03 % higher than in the starting material.

Table 7. Pharmaceutical technological parameters of samples containing iron(II) sulfate monohydrate and natural bed materials, produced by special hot melt technology

	Sample 1	Sample 2	Sample 3
Particle mass (mg)	**10.6** ± 0.001	**10.5** ± 0.002	**10.9** ± 0.002
Particle size (mm)	**1.792** ± 0.051	**1.998** ± 0.189	**1.776** ± 0.078
Particle's total $Fe(II)SO_4$ content (mg)	**6.41** ± 0.183	**6.97** ± 0.483	**6.15** ± 0.074
Particle's Fe^{3+} content (%)* *starting Fe^{3+} content: 0.40%	**0.42** ± 0.01	**0.43** ± 0.01	**0.43** ± 0.02

In vitro drug release studies

The in vitro release of iron (II) sulfate from the produced formulations was studied in different fluids, such as distilled water, artificial gastric fluid and phosphate buffer. The produced samples store iron in the solid state, incorporated in the lipophilic matrix. The iron(II) sulfate released from the matrices must be in the dissolved form in the stomach for effective absorption in the proximal intestine. Since the highest drug release was detected in the artificial gastric fluid with an acidic character, the in vitro release results for the artificial gastric fluid are shown (Fig. 15.).

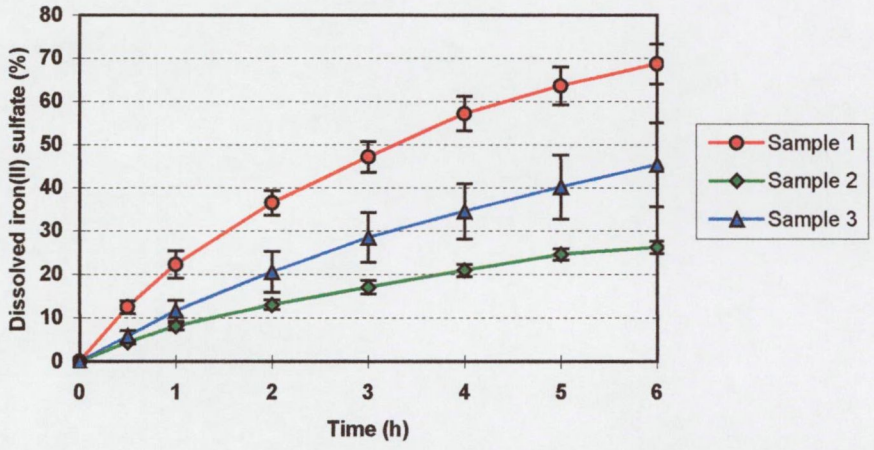

Fig. 15. In vitro dissolution of iron(II) sulfate in artificial gastric fluid at 37 °C, from samples 1 (o), 2 (◊) and 3 (Δ)

The rates of dissolution of the iron(II) sulfate from the various lipophilic matrices were basically low. However, considerable differences were observed in the amount of active agent liberated. The greatest quantity of iron(II) sulfate was dissolved from sample 1, i. e. 70% of the total iron content. This was followed by sample 3, with 45% release, and then sample 2, from which 26% of the total drug content was liberated during the study. In the in vitro tests, no significant differences

in drug release were detected between sample 2 and sample 3, whereas there were significant differences between sample 1 and sample 2, and between sample 1 and sample 3.

The in vitro test demonstrated that the rate of dissolution of the iron(II) sulfate was of approximately zero kinetic order with uniform release. The rate constants and the correlation coefficients (Table 8.) calculated in kinetic calculations confirm that the release of iron(II) sulfate was really zero order kinetic because there is no significant difference between the parameters of the two kinetic models, but the first order kinetic model in the case of sample 1 has a better correlation coefficient.

Table 8. Kinetic parameters of samples (based on in vitro experiments)

	zero-order model		**first-order model**	
	rate constant (k)	correlation coefficient (R)	rate constant (k)	correlation coefficient (R)
Sample 1	-8.3007	0.9768	-0.0839	0.9978
Sample 2	-3.4952	0.9843	-0.0220	0.9907
Sample 3	-4.9306	0.9905	-0.0435	0.9983

The drug release results in artificial gastric fluid are in accordance with the physico-chemical properties, and more particularly with the solubility properties of the iron(II) sulfate and the auxiliary materials. White wax and stearin are both insoluble in water and in acid medium, but stearin has an acid character and contains some water-soluble acid. Accordingly, the highest drug release was observed from sample 1, which contained stearin as bed material. The drug release was lower from sample 3, containing stearin and white wax, and the least from sample 2, which contained only white wax as bed material. The drug release profiles are in accordance with the surface of the samples, too.

In vivo experiments

A summary of the in vivo studies in rabbits is shown in Fig. 16. The curves demonstrate the increase in the plasma iron(II) concentration in comparison with the basic level measured before treatment. The points are the mean plasma iron(II) concentrations with the standard deviation in each group of 6 animals. As concerns the basic plasma iron level, no significant differences could be observed between the different groups.

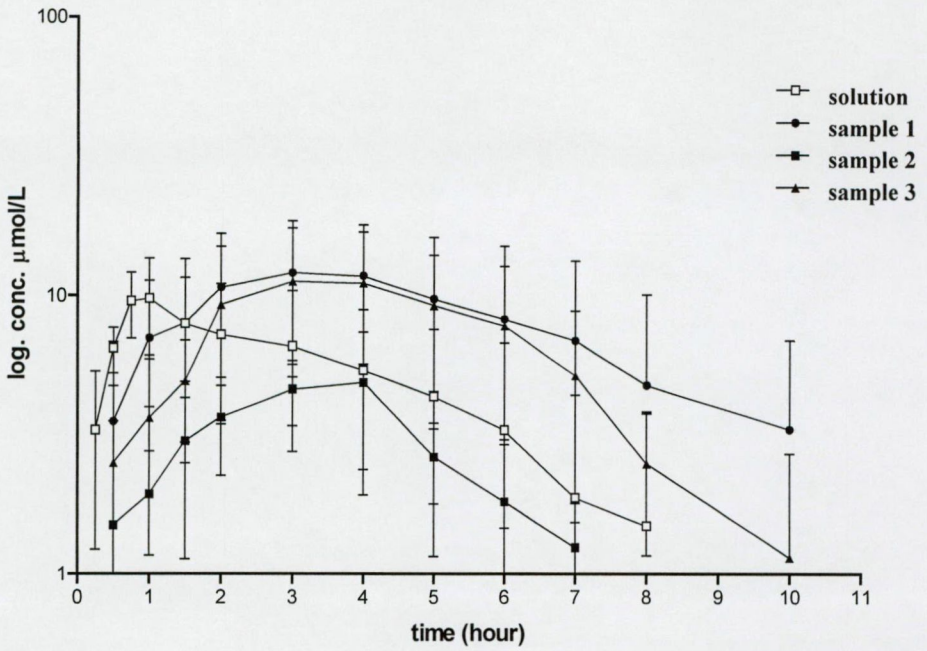

Fig. 16. Plasma iron levels in rabbits after oral administration of iron(II) sulfate-containing samples

The curves in Figure 16. reveal that the absorption was the fastest from the iron(II) sulfate solution administered as a control. The peak plasma iron(II) concentration (C_{max}) (9.77 ± 3.84 µmol/L) was reached within 1 h. For the three formulations studied, the absorption was considerably slower: the C_{max} values were measured 3 and 4 h after administration. The plasma level was 12.11 ± 6.43 µmol/L and 11.28 ± 6.16 µmol/L for sample 1 and 3, respectively. For the animals treated with sample 2, C_{max} was only 4.90 ± 2.52 µmol/L. As regards the three preparations, the lowest plasma iron concentrations were measured for sample 2, and these values fell to the normal level by 8 h.

The pharmacokinetic parameters determined from the curves are indicated in Table 9. The absorption half-life ($t_{1/2abs}$) for the iron(II) sulfate solution was 0.26 h, whereas it was 1.66 h for sample 1, 1.07 h for sample 2 and 1.40 h for sample 3. The difference was significant for each formulation. Significant differences in elimination half-life ($t_{1/2elim}$) were observed in relation to sample 2 and 3. However, no significant differences were found in mean residence time (MRT) between the solution (3.92 h) and the samples (5.19 h, 4.05 h and 5.06 h, for samples 1-3, respectively). The time to peak plasma concentration (t_{max}) was 1.07 h for the solution, in contrast with 3.06 h for sample 1, 2.58 h for sample 2 and 3.03 h for sample 3. The differences were significant.

The highest C_{max} was measured for sample 1 and 3 (13.88 and 12.41 μmol/L, respectively), followed by the aqueous solution (9.65 μmol/L) and sample 2 (5.58 μmol/L). The AUC values extrapolated to infinity were higher for sample 1 and 3 (95.6 μmol/L·h and 68.7 μmol/L·h) than for the solution (46.4 μmol/L·h), but the difference was significant only in the case of sample 1. The bioavailability relative to the iron(II) sulfate solution was 205.9%, 147.9% and 47.5% for sample 1, 3 and 2, respectively.

Table 9. Pharmacokinetic parameters calculated from plasma curves of rabbits after oral administration of iron(II) sulfate-containing samples

Treatment	Absorption half-life (h)	Elimination half-life (h)	MRT (h)	t_{max} (h)	C_{max} (μmol/l)	AUC∞ (μmol/l*h)	Bioavailability* (%)
Solution	**0.26**	**2.38**	**3.92**	**1.07**	**9.65**	**46.4**	**100.0**
(n=6)	± 0.10	± 0.46	± 1.25	± 0.22	± 3.60	± 34.4	
Sample 1	**1.66****	**1.84**	**5.19**	**3.06****	**13.88**	**95.6****	**205.9**
(n=6)	± 0.77	± 0.85	± 2.21	± 1.27	± 6.09	± 57.7	± 113.5
Sample 2	**1.07****	**1.42****	**4.05**	**2.58****	**5.58**	**22.1**	**47.5**
(n=6)	± 0.52	± 0.46	± 0.62	± 0.84	± 2.33	± 6.41	± 12.6
Sample 3	**1.40****	**1.60****	**5.06**	**3.03****	**12.41**	**68.7**	**147.9**
(n=6)	± 0.34	± 0.23	± 0.97	± 0.31	± 8.18	± 34.5	± 67.9

*bioavailability relative to solution (100%),
**mean difference related to solution is significant ($p<0.05$)

The results of the in vivo experiments indicate that all three formulations belong to the sustained-release category. The absorption half-lives of the products were significantly increased relative to that of the iron(II) sulfate solution, and the active agent reached the C_{max} statistically later for all three preparations. The highest C_{max} and AUC values were measured for the product produced with stearin (sample 1) and that containing stearin (sample 3). The kinetic parameters revealed that the best sustained-release preparation was the product which contained stearin as bed material.

The sustained release of the active agent led us to expect that the effect would be achieved without accompanying gastric irritation. To check on this, the gastric mucosa of the rabbits was examined after the in vivo study. After treatment with the iron(II) sulfate solution, considerable gastric irritation was observed (Fig. 17.) as a result of the iron reaching the stomach suddenly in a high concentration. However, no gastric irritation was noticed after the in vivo treatment of the three samples (Fig. 18.).

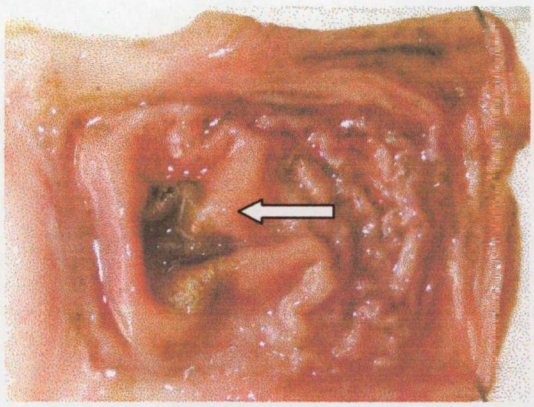

Fig. 17. Gastric mucosa after treatment with iron(II) sulfate solution

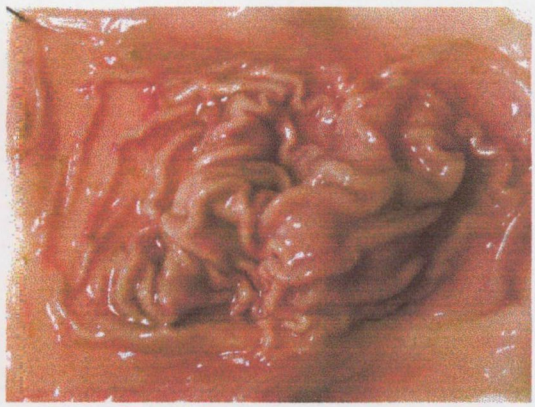

Fig. 18. Gastric mucosa after treatment with sustained release preparation (sample 3)

In vitro/in vivo correlation

The *in vitro/in vivo* correlations for the three formulations were explored by comparing the *in vivo* drug release obtained from deconvolution with the *in vitro* release data [125]. The results in Figure 19. indicate approximately linear correlations between the *in vivo* and the *in vitro* fractional release for the matrix systems. The slopes and the intercepts obtained from the pooled data for the three formulations suggested that the overall *in vitro* release is faster than the *in vivo* release.

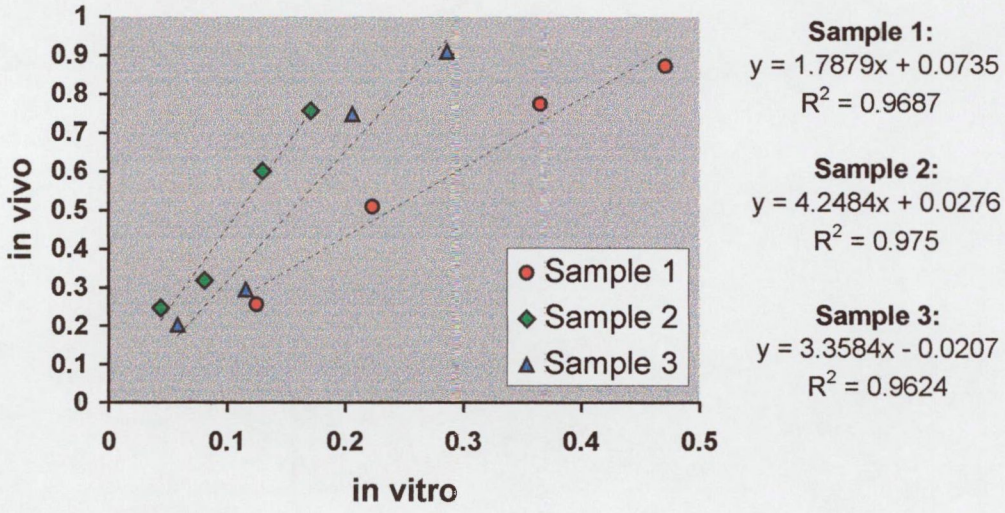

Fig. 19. In vitro/in vivo correlation based on pooled data of samples produced with special hot melt technology

Morphological analysis

These investigations related in part to the properties of the particles (before and after administration) and in part to the potential irritation of the gastric mucous of the rabbits.

The electron microscopic pictures showed that each particle has a spherical form with a more or less even and continuous surface. The quality of the surface was crucially determined by the bed materials.

Sample 1, prepared with stearin (Fig. 20.), has an uneven surface with cracks in it (Fig. 20a). The iron liberation is presumed to be accelerated by dissolution through these cracks. After the animal tests, the particles in the stomach of the animals were found to be unbroken, i.e. the particles did not disintegrate *in vivo*. The auxiliary agent remained as a framework keeping the spherical shape, but superficial changes were noted. The surface became even, the cracks disappeared (Fig. 20b) and recrystallization of the stearin could be observed (Fig. 20c).

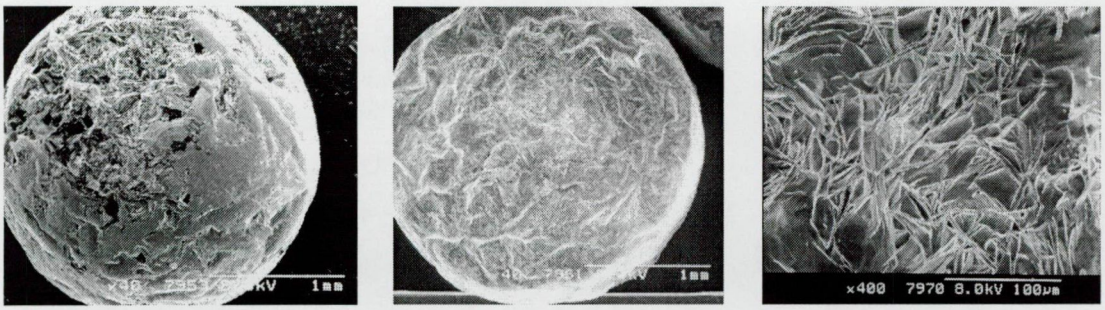

a **b** **c**

Fig. 20.: Electron microscopic pictures of sample 1 (bed material: stearin): surface of the intact particle (**a**), surface of the particles after the in vivo study (**b**, **c**)

For sample 2, prepared with white wax (Fig. 21.), the particle surface was completely smooth, and no cracks were noted (Fig. 21a). Sample 2 had a more compact structure than that of sample 1. The particles remained unbroken after the *in vivo* study, but traces of superficial erosion (Fig. 21b) and iron(II) sulfate aggregation on the surface (Fig. 21c) could be observed.

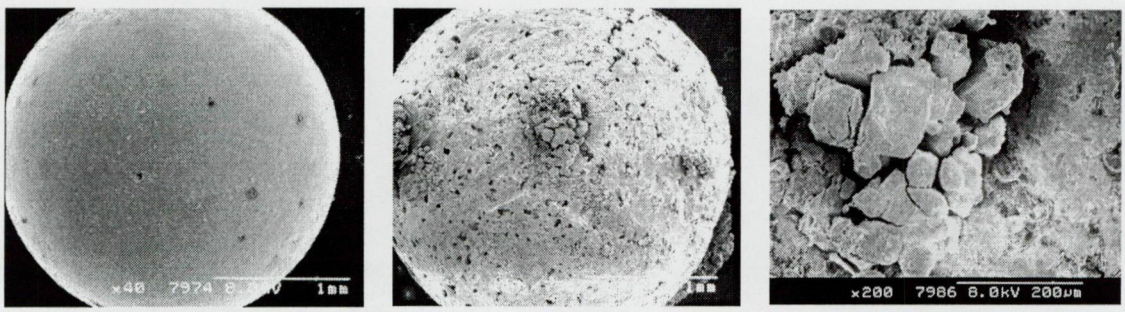

a **b** **c**

Fig. 21.: Electron microscopic pictures of sample 2 (bed material: white wax): surface of the intact particle (**a**), surface of the particles after the in vivo study (**b**, **c**)

Sample 3, which contained both of the bed materials, also had a smooth, even surface (Fig. 22.). The explanation of this even surface is that a mixture of stearin and white wax in a ratio of 1:1 was used and the white wax corrected the roughness of the surface (Fig. 22a). After the animal tests, the particles found in the stomach of the animals had a spherical shape, but the surface had become uneven as a result of the dissolution of iron(II) sulfate (Fig. 22b). After the *in vivo* study, the particles exhibited a spongy structure (Fig. 22c).

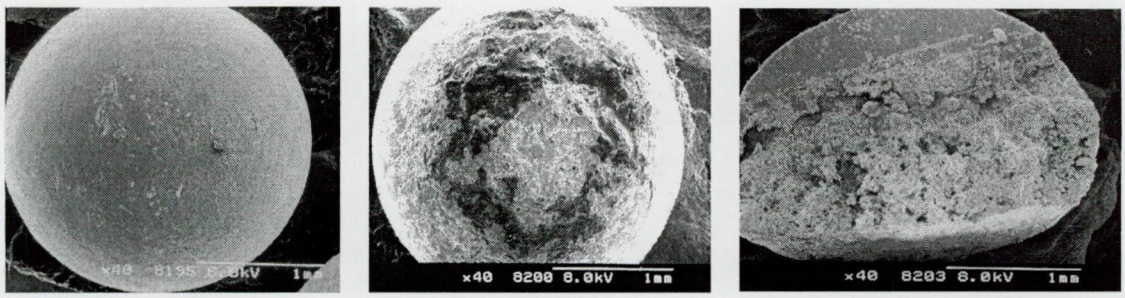

a **b** **c**

Fig. 22.: Electron microscopic pictures of sample 3 (bed material: stearin and white wax): surface of the intact particle (**a**), surface of the particle after the in vivo study (**b**), cross-section of the particle after the in vivo study (**c**)

The samples were submitted to the X-ray powder diffraction assay to establish the effect of the heat-treatment related to the special hot melt technology in the structure of the bed materials. The test shows that no structural change occurred in the stearin and white wax during the processing.

5.2.2 Use of semisynthetic bed materials (glycerine derivatives) in the melt technology

Iron(II) sulfate containing solid matrices were developed with special hot melt technology also with the use of new and modern auxiliary materials such as glycerine derivatives. The bed materials were Compritol ATO 888® (glyceryl-behenate) and Precirol ATO 5® (glyceryl-palmitostearate).

Pharmaceutical technological evaluation of samples

The melt technology resulted in round particles again. Two new samples signed as sample 4 (Compritol ATO 888®) and sample 5 (Precirol ATO 5®) were produced with glycerine derivatives. The results of the pharmaceutical technological evaluation of the samples are presented in Table 10.

Table 10. Parameters of iron(II) sulfate monohydrate containing samples produced with glycerine derivatives as bed material(the composition is shown in Table 6.)

	Sample 4	Sample 5
Particle mass (mg)	**13.18** ± 0.003	**12.74** ± 0.003
Particle size (mm)	**2.2** ± 0.227	**2.1** ± 0.121
Particle's total $Fe(II)SO_4 \bullet H_2O$-content (mg)	**5.08** ± 0.128	**5.49** ± 0.082
Particle's Fe^{3+} content (%)* *starting Fe^{3+} content: 0.40%	**0.42** ± 0.020	**0.43** ± 0.020

The mean mass of the particles is almost the same in the new products. In comparison with the other samples (sample 1-3), the particle sizes of sample 4 and 5 are greater. The mean particle mass is about 13 mg and their diameter is more than 2 mm.

The particles contain an average amount of 5 mg iron(II) sulfate monohydrate. This iron content is lower than the content of samples 1-3. The difference between the mass, size and iron content can be explained by the different drop forming properties and viscosity and by the different density of glycerine derivatives and the natural bed materials, such stearin and white wax. Oxidation was also low during the production, it was not more than 0.02-0.03% in comparison with the initial Fe^{3+}-amount. The low standard deviations support the reproducibility of production with this technology.

In vitro drug release study

The glycerine derivatives slowed the drug release in the in vitro drug release test (Fig. 23.). The rates of dissolution were different but fundamentally low in both cases. A greater quantity of iron(II) sulfate was dissolved from sample 4 (which contained Compritol ATO 888® as bed material), 45% of the total iron content was liberated. This liberation was the same as the drug liberation from sample 3, which disposed the best in vitro and in vivo properties in the first part of our investigation. From sample 5, 22% of the total drug content was liberated during the study. This is similar to the drug liberation from sample 2, which contains only white wax and showed the worst properties. However, the standard deviations were lower, and this indicates more uniform iron release from sample 4 and 5.

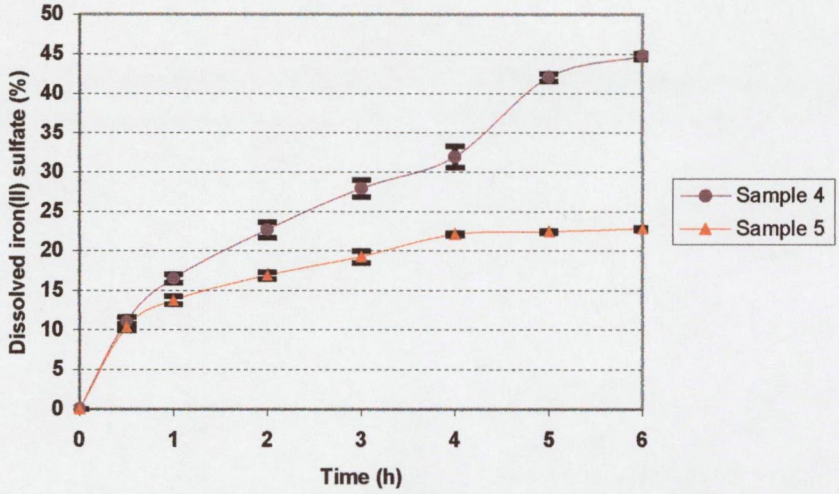

Fig. 23. In vitro dissolution of iron(II) sulfate in artificial gastric fluid at 37 °C, from samples 4 and 5

The kinetic calculation demonstrated that the release of iron(II) sulfate from sample 4 occurred according to zero order kinetics. The calculated rate constants and correlation coefficients are shown in the Table 11. On the basis of these values, drug liberation from sample 5 cannot be described either as zero or as first order kinetics.

Table 11. Kinetic parameters of samples (based on in vitro experiment)

	zero-order model		**first-order model**	
	rate constant (k)	correlation coefficient (R)	rate constant (k)	correlation coefficient (R)
Sample 4	-6.8263	0.9770	-0.0401	0.9874
Sample 5	-3.1372	0.8760	-0.0159	0.8942

The results of pharmaceutical technological evaluation, the in vitro drug release test and the kinetic calculations confirm that glycerine derivatives are applicable in the melt technology as new and modern bed materials and are able to produce a solid dosage form with slow drug release. There were no in vivo tests with sample 4 and 5.

Morphological investigations were also performed. The stereo microscopic picture of sample 4 (Fig. 24a) shows homogeneous particle size distribution and round particle shape. The surface is even and smooth. The electron microscopic pictures reveal a continuous surface (Fig. 24b) composed by Compritol ATO 888®, which is a bit puckered (Fig. 24c).

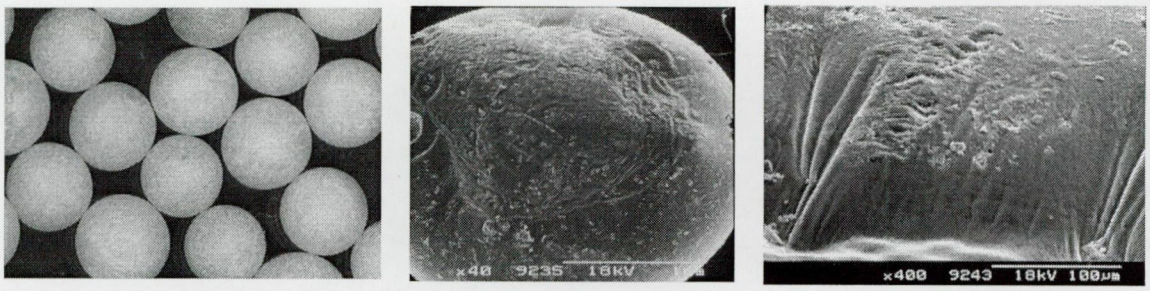

a **b** **c**

Fig. 24. : Stereo microscopic (**a**) and electron microscopic (**b, c**) pictures of sample 4 which contains iron(II) sulfate and Compritol ATO 888®

The stereo microscopic picture of sample 5 (Fig. 25a) produced with Precirol ATO 5® also shows round particles with homogeneous particle size. A more and less even surface (Fig. 25b) can be seen in the electron microscopic pictures, but this surface is not continuous, crystals can be observed (Fig. 25c).

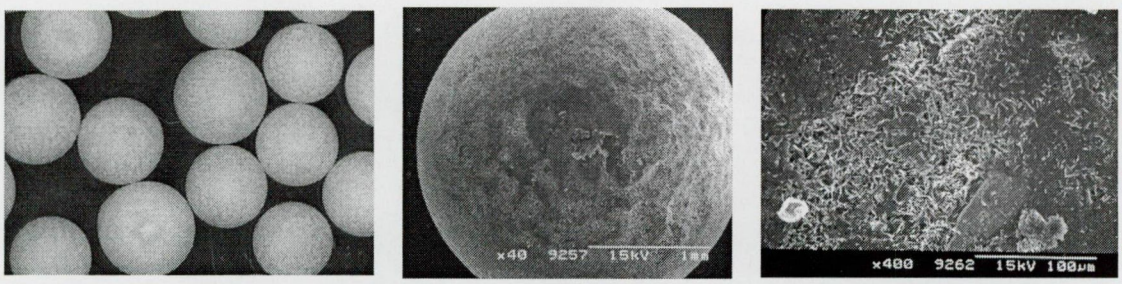

a **b** **c**

Fig. 25. Stereo microscopic (**a**) and electron microscopic (**b, c**) pictures of sample 5 which contains iron(II) sulfate and Precirol ATO 5®

The effect of heating during the process of special hot melt technology in the structure of auxiliary materials was checked with X-Ray powder diffraction assay. The analysis of Compritol ATO 888® showed two characteristic peaks with different intensity (Table 12). The repeated test after the hot melt process shows a decrease of 15% in the crystalline phase, which indicates structural realignment upon the effect of heating accompanying the process. The X-ray powder diffractogram of Precirol ATO 5® shows 4 typical peaks, two of which occur at the 2Θ value characteristic of Compritol ATO 888®. The counts's number related to the angles of incidence clearly indicates that heating effects a greater change in the structure and in the crystalline-amorphous ratio in Precirol ATO 5® than in Compritol ATO 888®. This change can probably be related with the difference observed in the in vitro drug release.

Table 12. The crystalline and the amorphous rate in glycerine derivatives

	Compritol ATO 888®- before heating				Compritol ATO 888®-after heating				Change** (%)
2 Θ [°]	21.090		23.095		21.080		23.025		
Crystalline part [cps]*	63152		16615		55131		13619		**-15.37**
Amorphous part [cps]	6889		6273		5806		6593		**-10.62**
	Precirol ATO 5®-before heating				**Precirol ATO 5®-after heating**				
2 Θ [°]	5.355	19.370	21.105	22.820	5.280	19.385	21.165	23.170	
Crystalline part [cps]	4984	22530	23409	23470	4570	13502	30102	17450	**-11.36**
Amorphous part [cps]	1584	3249	3540	3832	1616	4844	4858	4886	**+28.96**

*cps= counts per secundum

** mean change, calculated from cps related to the 2Θ values

5.2.3 Conclusion

The results confirm the applicability of the special hot melt technology in the production of iron(II) sulfate-containing drop-formed particles with round shape. The processing of iron is achievable successfully using lipophilic skeleton-building materials with a low melting temperature. The conventional natural materials (stearin and white wax) and the new auxiliary materials of pharmaceutical technology (Compritol ATO 888®, Precirol ATO 5®) are also applicable. The production of samples with special hot melt technology is well reproducible, quick and cost-saving. Iron is not oxidized notably during the process.

The conventional natural materials ensure the iron release from samples according to zero order kinetics. The in vivo experimental results in rabbits correlate well with the results of the in vitro tests. The samples have good bioavailability.

The investigations with glycerine derivatives confirm the applicability of such materials in modern iron-processing. They slow down iron release, and the liberation of the active agent can be regulated by using their sufficient amount and with the addition of other materials. The bed materials form a matrix in the products, protect the iron from oxidation and ensure slow drug release.

It can be stated that drop solidification from the melt is suitable to produce a solid product with sustained drug release. The regulation of drug release in this manner can be advantageous especially in the case of gastric-irritating active agents like iron(II) sulfate.

5.3 Results 2-Experimental results of iron(II) sulfate samples produced with spherical crystallization

Crystallization from solution is a possibility to produce iron(II) sulfate crystals which are suitable for formulating a new solid dosage form. The spherical crystals produced in this way have several advantages, which facilitate further production steps (e.g. coating) and the formation of the final dosage form.

Results of the preformulation studies

Different samples were produced during the preformulation studies and were examined parallelly. 11 crystallized samples (signed as Fe/2 – Fe/11) were produced by changing the process parameters (Table 13.). The production and the testing were performed in two parts.

Table 13. Crystallization parameters of iron(II) samples (Fe/2-Fe/11) in preformulation studies

Sample	T_s (°C)	V_C (°C/min)	Cooling method	n (min^{-1})	Solvent	M_s (g)	
Fe/2	54	0.35	lin.	600	tap water	6	First part
Fe/3	54	1.3	lin.	600	tap water	0	
Fe/4	58	varying	exp.	600	tap water	0	
Fe/5	58	varying	exp.	600	distilled water	0	
Fe/6	58	0.33	lin.	800	distilled water	0	
Fe/7	58	0.33	lin.	800	distilled water	0	
Fe/8	58	[1]0.55 [2]0.2	lin.	800	deionized water	0	Second part
Fe/10	58	0.28	lin.	800	deionized water	0	
***Fe/11**	58	0.17	lin	800	deionized water	0	

T_s= starting temperature, V_C= cooling rate, **n**= agitation speed, M_s= seed crystal
[1] between 0 and 60. min.
[2] between 60. and 135. min.
* + 1 hour mixing after the end of crystallization (15 °C)

The particle size distribution, the time of flow (flowability), the bulk density and the roundness of the crystallized samples were tested. From the economic point of view, a requirement of the produced crystals is that the size of most of the particles should be between 0.5 and 1.0 mm because these crystals can be used for coating.

In the first part of the preliminary study (Table 13.) those experiments gave the best result in which a starting temperature of 58 °C, a linear cooling method, an agitation speed of 800 l/min and no seeding were applied. Using these parameters in the second part, the effect of cooling rate was examined and deionized water was used to avoid the effect of solvent ions. The ions can disturb nucleation and crystal growth, and thus the reproducibility of crystal production. The parameters of crystallized products in the second part are presented in Tables 14. and 15.

Table 14. Particle size distribution of iron(II) sulfate samples (Fe/8-Fe/11) produced with spherical crystallization in the second part of preliminary studies

Sample	> 1.0 mm	1.0-0.8 mm	0.8-0.71 mm	0.71-0.5 mm	0.5-0.4 mm	< 0.4 mm
Fe/8 (g)	0.1	0.1	3.6	34.0	19.4	42.8
Fe/10 (g)	1.3	12.2	11.5	41.1	15.7	18.2
Fe/11 (g)	38.3	18.6	9.4	23.6	5.9	4.2

Table 15. Time of flow, bulk density and roundness of the crystallized products

Sample	Time of flow ($s/100\ cm^3$)	Bulk density (g/cm^3)	Roundness
Fe/8	8	0.943	1.46 ± 0.26
Fe/10	8	0.971	1.32 ± 0.12
Fe/11	10	1.010	1.21 ± 0.09

There are no significant differences in the samples with respect to their bulk density and roundness. Their flowability was proper based on the time of flow. Sample Fe/10 was the best as concerns particle size distribution, but the best values for roundness, standard deviation of roundness and bulk density were given by sample Fe/11 produced with the smallest cooling rate.

The crystal-water content of the produced samples was tested with thermoanalytical examinations and it was calculated from the decrease of sample mass. The water content determined was the following: Fe/8: 6.27 mol, Fe/10: 6.88 mol, Fe/11: 6.70 mol H_2O.

Results of the scale up process

A fivefold scaled up experiment was executed by applying parameters found to be the best in laboratory (Fe/11) experiments. The recrystallization was performed in deionized water with no addition of seed crystals and by cooling in a linear manner, with 0.2 °C/min cooling rate. Agitation rate was adapted to the larger scale in order to

yield similar mixing to the lab experiment: it was decreased from 800 to 400 min^{-1}. The composition of solution was: 1.81 kg $FeSO_4 \cdot 7H_2O$ and 1.35 kg deionized water. The particle size distribution of crystals produced in the best laboratory experiment (Fe/11) and the scaled up crystallization (Fe/12) is compared in Figure 26.

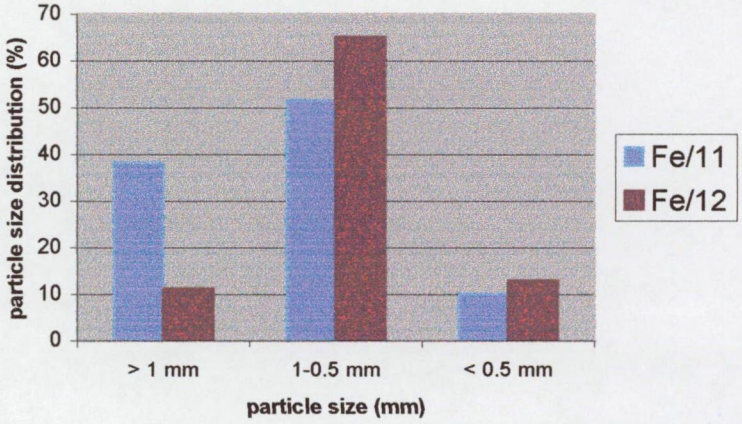

Fig. 26. Particle size distribution of samples Fe/11 and Fe/12

Data in Figure 26. show that scale up effected an improvement in the particle size distribution. The rate of samples in the range of 0.5 - 1 mm increased, more than 60% of Fe/12 belongs to this range. Thus the scale up process was expressly favourable with respect to particle size. The other characteristics (mean diameter, time of flow, bulk density, roundness) of Fe/12 in comparison with Fe/11 are shown in Table 16.

Table 16. The comparison of the pharmaceutical technological parameters of samples Fe/11 and Fe/12

Sample	Mean diameter (μm)	Time of flow (s/100 cm^3)	Bulk density (g/cm^3)	Roundness
Fe/11	734 ± 183	10	1.010	1.21 ± 0.09
Fe/12	729 ± 165	8	0.994	1.32 ± 0.11

The flowability of sample Fe/12 did not change greatly, the bulk density decreased slightly and the roundness became slightly worse but it was still satisfactory. However, these changes are not significant and sample Fe/12 was given good classification.

Morphological analysis

The images of the iron(II) sulfate heptahydrate available in trade and developed by means of spherical crystallization are demonstrated by stereo

microscopic pictures. The iron(II) sulfate available on the market (Ph. Hg. VII.) is greatly heterogeneous, the crystal shape is diverse (Fig. 27.). As concerns the crystal habit, crystals are mainly monoclinic but orthorombic crystals can also be found, which is in agreement with the data in literature. The crystal surfaces are white and matt, which leads to the conclusion that crystal crumbling occurred due to the effect of the atmosphere.

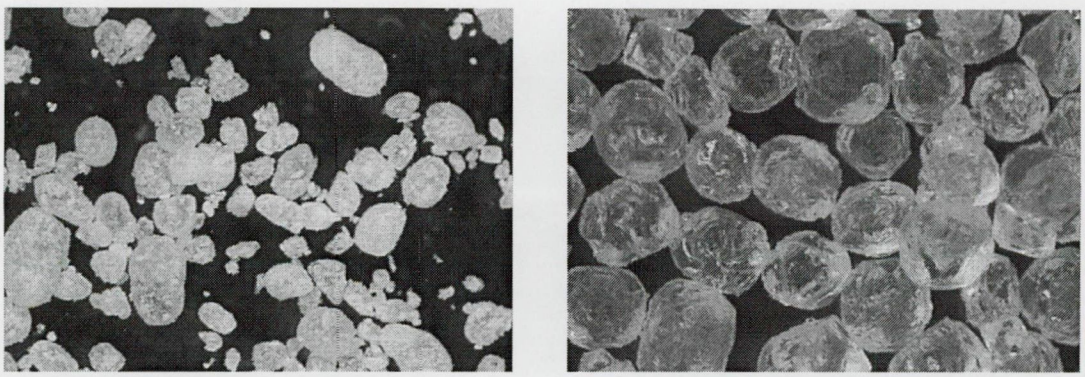

a. (size range: 10 μm-2 mm) **b.** (size range: 0,5-1,0 mm)

Fig. 27. Stereo microscopic pictures of iron(II) sulfate heptahydrate crystals available in trade (**a**) and developed (**b**)

The crystals of sample Fe/12 developed by spherical crystallization from solution are like glass, semitransparent with sea-green colour and their shape is approximately round. The conventional BCC-cubic structure of crystals is transformed into a rounded, spherical form owing to the parameters of the crystallization process.

Crystal-coating process

The aim was partly to prove that the spherical crystals can be coated fast and easily, and partly to form a coat on the particles which can control the release of iron(II) sulfate. The starting material was 100 g from the 0.5-1 mm fraction of sample Fe/12. The coating experiments were performed in all three cases in a steel pan with the spraying method in such a way that the same amount of iron(II) sulfate was treated with various amounts of stearin. Spraying was carried out with a solution of stearin in 95% ethyl alcohol having a temperature of 60 °C. The composition of the coated products (HPT-1, HPT-2, HPT-3) is shown in Table 17.

Table 17. The composition of the coated samples.

		HPT-1	HPT-2	HPT-3
Amount of $FeSO_4*7\ H_2O$ (g)		100	100	100
Composition of the final product*:	Iron(II) sulfate heptahydrate (%)	95.5	89	72
	Amount of stearin (%)	4.5	11	28

* The determination of iron was performed by atomic absorption method at 248.3 nm in air-acetylene gas after a burning process (500 °C, 24 h).

The difference between the samples concerning the quantity of iron(II) sulfate heptahydrate and stearin is illustrated clearly by the data in Table 17.

Investigation of coated samples

The particle size distribution of coated samples (HPT-1, HPT-2, HPT-3) is demonstrated in Figure 28. It is obvious that the particle size distribution of the coated products changes parallelly with the increase in the quantity of stearin. With increasing amounts of stearin, the ratio of particles larger than 1 mm increased, while the ratio of particles belonging to the 0.5-1 mm range and smaller than 0.5 mm decreased.

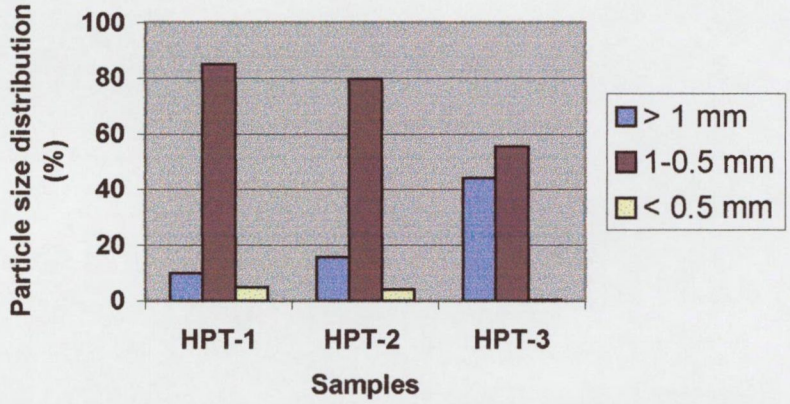

Fig. 28. Particle size distribution of coated iron(II) sulfate heptahydrate samples

The roundness and diameter values of both the starting and the coated particles are shown in Table 18. The data in Table 18. correlate well with the data of Figure 28. in the sense that the mean diameter of samples increased proportionally with the amount of stearin. The roundness values were also changed but improvement was found only in the case of samples HPT-1 and HPT-3, and the 11% of stearin used as coating material in sample HPT-2 did not modify the roundness of the starting material.

Table 18. Parameters of the starting and the coated particles

	Starting $FeSO_4*H_2O$	HPT-1	HPT-2	HPT-3
Roundness (Leica)	1,32 ± 0,11	1,27 ± 0,11	1,32 ± 0,08	1,19 ± 0,05
Diameter (Leica) (µm)	729 ± 165	768 ± 173	782 ± 172	894 ± 152

In vitro drug release study

The rate of dissolution of the active agent from coated products in artificial gastric juice is illustrated in Figure 29. The values are expressed in the amount of iron(II) sulfate heptahydrate and are related to the maximum releasable active agent content in percentage.

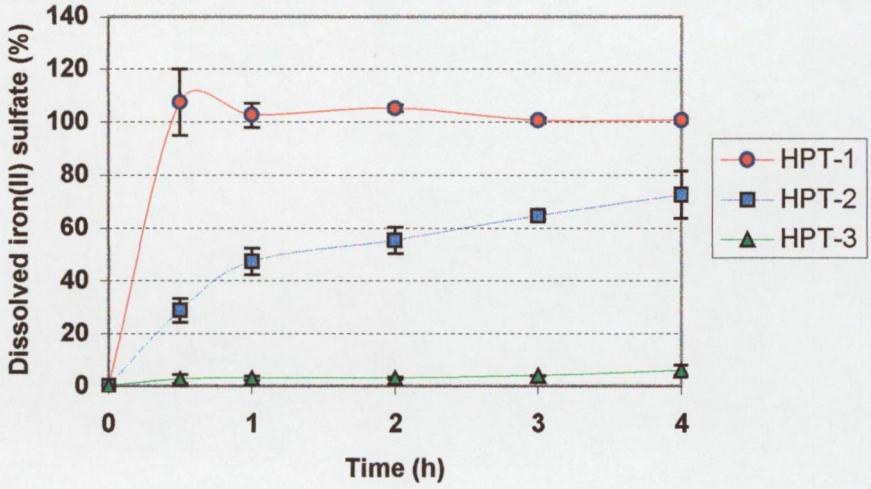

Fig. 29. In vitro drug release of coated samples in artificial gastric juice

The liberation of the active agent from samples coated with different amounts of stearin was found to be significantly different. The total iron content was liberated from the sample HPT-1 during the first 0.5 hour of study. It can be seen in the diagram that the values measured at the beginning of the study exceeded 100 %. The value of 107.5% and the high standard deviation which appeared at the 0.5 hour indicate the insufficient mixing of the system. The solution was not homogeneous after 30 minute. This is also supported by the fact that the amount of released iron(II) sulfate became "steady" around 100% in time, and at the same time the standard deviation values decreased. This indicates that the system became homogeneous at the end of the dissolution test. The drug release from sample HPT-2 was uniform, in the 0.5 hour 28.8 % of the active agent was detected and 72.6 % of the total drug content

was liberated during the study. From sample HPT-3 the whole liberation was only 6%. Kinetic calculations were also performed on the basis of the results of the in vitro dissolution test (Table 19.).

Table 19. Kinetic parameters of coated iron(II) sulfate heptahydrate samples

	zero-order model		first-order model	
	rate constant (k)	correlation coefficient (R)	rate constant (k)	correlation coefficient (R)
HPT-1	-	-	-	-
HPT-2	-15.717	0.9085	-0.130	0.9481
HPT-3	-1.161	0.9124	-0.005	0.9189

Sample HPT-1 cannot be described either as zero or as first order kinetics because of the fast drug liberation. The correlation coefficients of HPT-2 and HPT-3 calculated according to the two kinetic models are similar. The rate constant belonging to HPT-2 considering the rise of the curve indicates a value similar to that of Sample 1, produced with special hot melt technology. In view of this, sample HPT-2 can be expected to have the best bioavailability.

Morphological investigation

Stereo microscopic pictures are shown in Figure 30. Sample HPT-1 has a favourable roundness compared to the roundness of the uncoated crystals. Stearin, used in as small an amount as 4.5%, levels off the unevenness of particles by sticking to surface holes but this amount is not sufficient to form an even, properly thick layer on the surface of crystals. As a consequence, release of the active agent from the sample is too fast. The roundness of sample HPT-2 is equal to the roundness of the uncoated crystals. In this sample stearin, which was applied in 11% compared to iron(II) sulfate, covers the entire surface of particles with an evenly thick layer and does not change the shape and roundness of crystals. So the rate of dissolution of iron measured in vitro shows slow, properly sustained release. The roundness of crystals is improved (even better than the roundness of sample HPT-1), which can be attributed to the 28% of stearin used. The thick layer not only smoothes the surface of crystals but retards release of iron(II) sulfate exaggeratedly under in vitro circumstances.

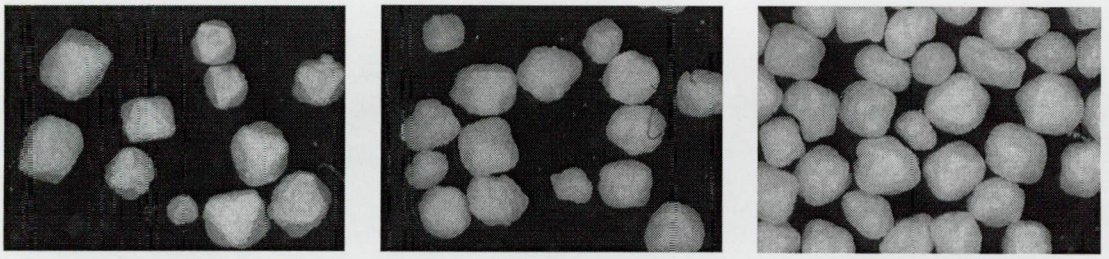

HPT-1 (mean diameter:768 μm) **HPT-2** (mean diameter:782 μm) **HPT-3** (mean diameter:894 μm)

Fig. 30. Stereo microscopic pictures of iron(II) sulfate heptahydrate crystals coated with stearin

5.3.1 Conclusion

The following statements can be made in connection with the spherical crystallization of iron(II) sulfate heptahydrate and the coating of developed crystals: With the use of non typical spherical crystallization in lab experiments, spherical iron(II) sulfate heptahydrate crystals were developed with a mean diameter of 0.5-1 mm. The procedure is simple, fast and does not require a dangerous, expensive solvent. In a fivefold scaled up experiment the desired requirements of particles were achieved. The size and the surface of the spherical crystals were suitable for coating. The coating procedure was developed for coating the surface of particles prepared by crystallization. The rate of iron(II) sulfate release was influenced by the thickness of the stearin layer. As a result of our development, the filling of spherical crystals into capsules to form the final dosage form can be proposed.

6. Summary

The aim of my PhD work was to prepare a solid dosage form from different hydrate forms of iron(II) sulfate using the melt solidification in drops method (special hot melt technology) and the non typical spherical crystallization process. These are new technologies in the field of pharmaceutical technology and have not been used before.

I acquired the technology of melt solidification in drops in Germany, in the Institute of Process Engineering of Martin Luther University, Halle-Wittenberg. After the preformulation studies (contact angle measurement, determination of surface free energy etc.) this method is suitable for the fast and simple preparation of the solid

product in one production step. The produced particles are round with a definite particle size.

Another advantage is that the liberation of the active agent is regulated at the same time, but it can be used only in the case of thermoresistant drugs. The first finding in the course of my investigations was that iron(II) sulfate monohydrate is suitable for the special hot melt technology because of its greater resistance during the heating process.

The spherical crystallization of iron(II) sulfate was attained with the help of crystallizer specialists of EGIS pharmaceutical company. Iron(II) sulfate can be crystallized from solution in a heptahydrate form. This method is applicable well if the aim is to give shape and to change the crystal habit already in the course of raw material manufacturing. After the establishment of the adequate parameters of the crystallization process, crystals with a defined particle size can be produced.

The results of my investigations concerning the working-out of both technologies are the following:

⇒ I found that the results of the samples developed by special hot melt technology confirm the applicability of this method in iron processing. The production of iron-containing solid particles is fast, simple and well reproducible. Natural auxiliary materials such as stearin and white wax are well applicable in the production, they protect the active agent and ensure slow drug liberation. The slow drug release means prolonged drug effect and uniform drug plasma concentration in the body together with the decrease of the risk of gastric mucosa irritation. The oxidation of iron was reduced, the increasing of the Fe^{3+}content in samples was minimal compared to the starting material.

⇒ Moreover, I found that spherical iron(II) sulfate heptahydrate crystals can be crystallized from solution with the use of the non typical spherical crystallization process. The production of spherical crystals is simple and fast if the parameters of crystallization are optimized. I developed the crystal coating process. The produced coat from stearin protects the iron from oxidation and inhibits the loss of crystal water. Drug liberation can be prolonged through the coat.

The production of solid dosage form (tablet, capsule) from iron compounds with conventional present-day technologies is difficult and circuitous. Production consists of several production steps, all of which are expensive and require a long

time. With the use of the special hot melt technology and the non typical spherical crystallization process, a solid dosage form suitable for direct peroral administration can be produced from iron(II) sulfate in a fast and simple manner (Fig. 31.).

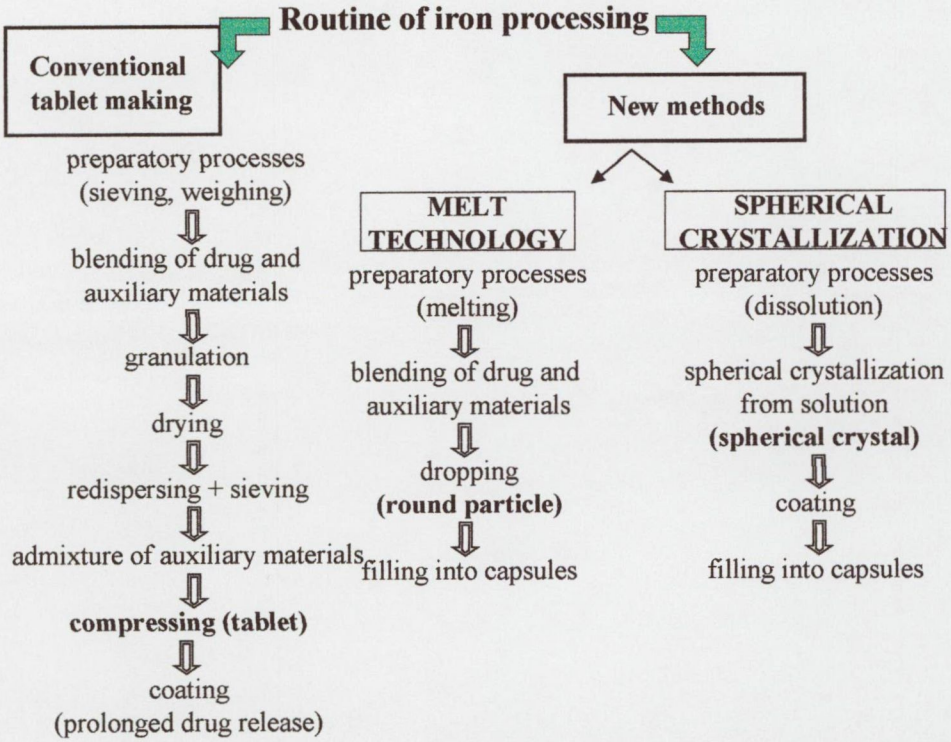

Fig. 31. The routine of iron processing with conventional and new methods

On the basis of my investigations both the special hot melt technology and the non typical spherical crystallization process are suitable for the production of solid dosage forms from iron(II) sulfate. The technological course of processing is shortened by these methods. The filling of round particles is suggested first of all into capsules, thereby forming a modern and popular final dosage form.

This study was supported by the Cultural Ministry of Sachsen-Anhalt (Germany), the Hungarian Research Fund (OTKA-T032707, OTKA-T047166), the German Scientific Academy and the Hungarian Scolarship Committee (DAAD-MÖB project 2000/2001, No. 58, and DAAD-MÖB project 2003/2004, No. 4).

7. References

[1] Bálint P., Orvosi élettan, Medicina, Budapest (1972) p. 78.

[2] Goodman and Gilman's The pharmacological basis of therapeutics (10th ed.), J. G. Hardman, L. E. Limbird, A. Goodman Gilman, McGraw-Hill, Toronto (2001) pp. 1317-1325.

[3] H. Tapiero, L. Gaté, K. D. Tew, Biomed. Pharmacoter. 55 (2001) 324-332.

[4] Szollár L., Kórélettan, Semmelweis Kiadó, Budapest (1993) pp. 36-38.

[5] Iron nutrition in health diseases, L. Hallberg, N. G. Asp (Eds.), John Libbey and Co. (1996) pp. 165-182.

[6] Iron nutrition in health diseases, L. Hallberg, N. G. Asp (Eds.), John Libbey and Co. (1996) pp. 137-148.

[7] W. F. Ganong, Az orvosi élettan alapjai, Medicina, Budapest (1995) pp. 493-494

[8] Sas G., www.medlist.com/HIPPOCRATES/II/4/228.htm

[9] Sas G., Nemesánszky E., Bräuer H., Scheffer K., Drug Research, 34 (1984) 1575-1579.

[10] Fürst Zs., Gyógyszertan, Medicina, Budapest (1998) pp. 602-606.

[11] R. S. Eisenstein, K. P. Blemings, J. Nutr. 128 (1998) 2295-2298.

[12] Ádám V., Dux L., Faragó Á., Fésüs L., Machovich R., Mandl J., Sümegi B., Orvosi biokémia, Medicina, Budapest (2001) pp. 262-264.

[13] G. N. Ioannou, J. Spector, K. Scott, D. C. Rockey, Am. J. Med. 113 (2002) 281-287.

[14] M. Schaefer, T. Reinecke, Sysmex Journal International, 11 (2001) 59-62.

[15] A. G. Greenburg, Am. J. Med. 101, suppl. 2A. (1996) 7-11.

[16] Gyógyszerkompendium, az Országos Gyógyszerészeti Intézet hivatalos kiadványa, MediMedia Információs Kft, Budapest (2002).

[17] Pallagi E., Szabóné Révész P., Erős I., Gyógyszerészet, 48 (2004) 332-338.

[18] Gmelins Handbuch der Anorganischen Chemie, Eisen, Teil B, die Verbindungen des Eisens, Nr. 59, Verlag Chemie GmbH., Berlin (1932) p. 401.

[19] F. Fraenckel, Dissert. Heidelberg (1905) p. 17-34.

[20] Gmelins Handbuch der Anorganischen Chemie, Eisen, Teil B, die Verbindungen des Eisens, Nr. 59, Verlag Chemie GmbH., Berlin (1932) p. 404.

[21]Ulmann's Encyclopedia of Industrial Chemistry, 5th Ed., Vol. A 14, B. Elvers, S. Hawkins, M. Ravenscroft, G. Schulz (Eds.), VCH Verlagsgesellschaft mbH, Weinheim (1989) p. 591.

[22] Kristályok geometriai leírása-surph.fat.bme.hu/pub/fizika

[23] F. S. Beudant, Ann. Chim. Phys. 4 (1817) p. 78.

[24] W. H. Wollaston, Ann. Chim. Phys. 7 (1817) p. 394.

[25] V. R. v. Zepharovich, Ber. Wien. Akad. 79 (1879) p.189.

[26] H. E. Armstrong, E. H. Rodd, Pr. Roy. Soc. A 90 (1914) p. 467.

[27] Kirk-Ottmer, Encyclopedia of Chemical Technology, 4th Ed., Vol. 14, John Wiley and Sons, USA (1995) p. 886.

[28] V. R. v. Zepharovich, Ber. Wien. Akad. 79, I. (1897) p. 189.

[29] H. E. Armstrong, E. H. Rodd, Pr. Roy. Soc. A 90 (1914) p. 467.

[30] W. T. Schaller, Bl. Depart. Geol. Univ. California, 3 (1903) p. 197.

[31] Y. G. Jeong, W. H. Jo, S. C. Lee, Polymer, 44, (2003) 3259-3267.

[32] C. Rosa, O. R. Ballesteros, M. Gennaro, F. Auriemma, Polymer, 44 (2003) 1861-1870.

[33]. K. Fukui, K. Maeda, Chemical Engineering Science, 57 (2002) 3133-3140.

[34] A. König, A. Schreiner, Powder Technology, 121 (2001) 88-92.

[35] O. Fischer, Chem. Ind. 83 (1986) 36-37.

[36] K. J. Kim, J. Ulrich, Powder Technology, 12 (2001) 81-87.

[37] G. Matz, Chem. Ing. Tech., 52 (1980) 570-575.

[38] H. C. Bülau, Dissertation, Schaker Verlag, Aachen (1999)

[39] J. Ulrich, Technische Kristallisation aus Lösung und Schmelze, Impulse 2, Universität Bremen (1987) 5-8.

[40] J. Ulrich, J. Bierwirth, Melt layer crystallization, Science and Technology of Crystal Growth, J. P. Eerden and O. S. L. Bruinesima (Eds.), Kluwer Academic Publishers, Dordrecht (Boston) London (1995) p. 248.

[41] J. Dredán, R. Zelkó, I. Antal, E. Bihari, I. Rácz, J. Pharm. Pharmacol. 50 (1998) 139-142.

[42] J. Breitenbach, Eur. J. Pharm. Biopharm. 54 (2002) 107-117.

[43] M. Doelker, M. Adel El-Egakey, M. Soliva, P. Speiser, Pharm. Acta Helv. 46 (1971) 31-52.

[44] Soliqs, The Drug Delivery Business of Abbott GmbH & Co KG, www.soliqs.com

[45] H. H. Gruenhagen, O. Mueller, Pharmaceutical Manufacturing International (1995) 167-170.

[46] Rácz I., Selmeczi B., Gyógyszertechnológia, 3. kötet, Gyógyszerformatan, Medicina Könyvkiadó Rt., Budapest (2001) pp. 404-405.

[47] R. Schreiber, C. Vogt, J. Werther, G. Brunner, Journal of Supercritical Fluids, 24 (2002) 137-151.

[48] J. Hamdani, A. J. Moës, K. Amighi, Int. J. Pharm. 245 (2002) 167-177.

[49] J. Dredán, R. Zelkó, I. Antal, E. Bihari, I. Rácz, Int. J. Pharm. 160 (1998) 257-260.

[50] T. Shaefer, P. Holm, H. G. Kristensen, Drug Dev. Ind. Pharm. 16 (1990) 1249-1277.

[51] D. Voinovich, B. Campisi, M. Moneghini, C. Vincenzi, R. Phan-Tan-Luu, Int. J. Pharm. 190 (1999) 73-81.

[52] C. M. Mc. Taggart, J. A. Ganley, A. Sickmueller, S. E. Walker, Int. J. Pharm. 19 (1984) 139-148.

[53] F. Zhou, C. Vervaet, J. P. Remon, Int. J. Pharm. 133 (1996) 155-160.

[54] D. Voinivich, M. Moneghini, B. Pertussi, J. Filipovic-Grcic, I. Grabnar, Int. J. Pharm. 203 (2000) 235-244.

[55] R. Thies, P. Kleinebudde, Int. J. Pharm. 188 (1999) 131-143.

[56] R. Thies, P. Kleinebudde, Eur. J. Pharm. Sci. 10 (2000) 103-110.

[57] P. Barthelemy, J. P. Laforêt, N. Farah, J. Joachim, Eur. J. Pharm. Biopharm. 47 (1999) 87-90.

[58] H. P. Huang, S. C. Mehta, G. W. Radebaugh, M. B. Fawzi, J. Pharm. Sci. 83 (1994) 795-797.

[59] J. Dredán, I. Antal, I. Rácz, Int. J. Pharm. 145 (1996) 61-64.

[60] Gombás Á., Szabóné Révész P., Erős I., Gyógyszerészet, 45 (2001) 299-304.

[61] H. Schnitzer, Verfahrenstechnik, 10 (1988) 30.

[62] A. Roberts, Chemie Technik, 25 (1996) 30-32.

[63] A. Roberts, Verfahrenstechnik, 30 (1996) 20-24.

[64] H. C. Bülau, A. Roberts, CRYSOPT Course on: Theory and Application of Melt Crystallization, 28.-29. Sept. 2000., Halle (Saale), Germany.

[65] Sandvik Process Systems, "Rotoform-Verfahren zur Herstellung von Pastillen", Die Chemische Production, 3 (1988) 50-52.

[66] P. J. Sell, A. W. Neumann, Angew. Chem. 6 (1996) 321-331.

[67] P. Grassmann, Physikalische Grundlagen der Verfahrenstechnik, Verlag Sauerländer, Aarau (1983) pp. 350-356.

[68] D. Li, M. Xie, W. Neumann, Colloid and Polimer Science, 271 (1993) 573-580.

[69] A. Hartwig, P. Wullf, Messen und Prüfen, 11 (1993) 90-92.

[70] U. Bröckel, F. Löffler, Part. Syst. Charact., 8 (1991) 215-221.

[71] www. kruss.de

[72] W. A. Zissman, Advances in Chemistry, 43 (1964) 1-51.

[73] F. M. Fowkes, Ind. Eng. Chem., 56 (1964) 40-52.

[74] D. K. Owens, R. C. Wendt, J. Appl. Polym. Sci., 13 (1969) 1741-1747.

[75] W. Rabel, Farbe und Lack, 77, 10 (1971) 997-1005.

[76] J. Schultz, K. Tsutsumi, J. B. Donnet, J. Coll. Int. Sci., 59 (1977) 272-276.

[77] J. Schultz, K. Tsutsumi, J. B. Donnet, J. Coll. Int. Sci., 59 (1977) 277-282.

[78] M. J. Schwuger, Lehrbuch der Gränzflächenchemie, Georg Thieme Verlag Stuttgart-New York (1996) pp. 110-123.

[79] Erős I., Gyógyszerészet, 26 (1982) 90-95.

[80] Pallagi E., Révész P., Erős I., Gyógyszerészet, 47 (2003) 83-90.

[81] Erdey Grúz T., A fizikai kémia alapjai IV., Műszaki Könyvkiadó, Budapest (1972) p. 209.

[82] T. Young, Philos. Trans, 95 (1805) 65.

[83] G. Matz, Kristallisation-Grundlagen und Technik, Springer Verlag, 2. Auflage, Berlin (1969).

[84] A. Mersmann, M. Löffelmann, Chem. Ing. Tech. 71 (1999) 1240-1244.

[85] A. Mersmann, Trans. IChemE., 74, Part A (1996) 812-820.

[86] A. Mersmann, K. Bartosch, J. Crystal Growth, 183 (1998) 240-250.

[87] J. A. Dirksen, T. A. Ring, Chem. Eng. Sci. 46 (1991) 2389-2427.

[88] J. W. Mullin, Crystallisation, 3rd Ed., Butterworths, London (1993).

[89] Y. Kawashima, M. Okumura, H. Takenaka, Science, 216 (1982) 1127.

[90] Y. Kawashima, M. Okumura, H. Takenaka, A. Kojima, Pharm. Sci., 73 (1984) 1535.

[91] H. Göcző, P. Szabó-Révész, B. Farkas, M. Hasznos-Nezdei, S. F. Serwanis, K. Pintye-Hódi, P. Kása jr., I. Erős, I. Antal, S. Marton, Chem. Pharm. Bull., 48 (2000) 1877-1881.

[92] P. Szabó-Révész, H. Göcző, K. Pintye-Hódi, P. Kása jr., I. Erős, M. Hasznos- Nezdei, B. Farkas, Powder Technology, 114 (2001) 118-124.

[93] S. Bhadra, M. Kumar, S. Jain, S. Agrawal, G. P. Agrawal, Pharm. Tech., 2 (2004) 66-76.

[94] Y. Kawashima, M. Okumura, H. Takenaka, Powder Technol., 39 (1984) 41-47.

[95] U. Löffler, R. Günther, T. Moest, Pharmazie, 48 (1993) 356-359.

[96] U. Löffler, A. Meyer, R. Günther, T. Moest, Pharmazie, 49 (1994) 665-671.

[97] K. Kachrimanis, G. Ktistis, S. Malamataris, Int. J. Pharm., 173 (1998) 61-74.

[98] Fürst Zs., Gyógyszertan, Medicina, Budapest (1998) pp. 102-105.

[99] H. M. Abdou, Dissolution, Bioavailability and Bioequivalence, Mack Printing Company, Easton, USA (1989) pp. 215-223.

[100] Pharmaceutics: The Science of Dosage Form Design, M. E. Aulton (Ed.), Churchill Livingstone Inc., USA (1988) 206-211.

[**101**] E. Pallagi, K. Vass, K. Pintye-Hódi, P. Kása Jr., G. Falkay,I. Erős, P. Szabó-Révész, Eur. J. Pharm. Biopharm. 57/2 (2004) 287-294.

[102] P. Barthelemy, J. P. Laforet, N. Farah, J. Joachim, Eur. J. Pharm. Biopharm., 47 (1999) 87-90.

[103] G. J. Vergote, K. Kiekens, C. Vervaet, J. P. Remon, Eur. J. Pharm. Sci. 17 (2002) 145-151.

[104] M. Juslin, I. Turakka, P. Puumalainen, Pharm. Ind., 42 (1980) 829-832.

[105] M. Grassi, D. Voinovich, M. Moneghini, E. Franceschinis, B. Perissutti, J. Filipovic-Grcic, J. Control. Rel. 88 (2003) 381-391.

[106] Magyar K., Általános farmakológia, SOTE Nyomda, Budapest (1996) 73-79.

[107] V. Ravelli, R. Rossi, Pharm. Manufact. Int. (1995) 171-172.

[108] J. J. Sousa, A. Sousa, M. J. Moura, F. Podczeck, J. M. Newton, Int. J. Pharm. 233 (2002) 111-122.

[109] Zs. Muskó, K. Pintye-Hódi, R. Gáspár, J. Pintye, P. Szabó-Révész, I. Erős, G. Falkay, Eur. J. Pharm. Biopharm. 51 (2001) 143-146.

[110] Barcza L., Buvári Á., A minőségi kémiai analízis alapjai, Medicina, Budapest (1997) p. 439.

[111] Burger K., A mennyiségi kémiai analízis alapjai. Műszeres elemzés, Medicina, Budapest (2000) p. 476.

[112] K. Ueno, T. Imamura, K. L. Cheng, Handbook of Organic Analytical Reagents, 2nd Edition (1992) p. 381.

[113] Rácz I., Selmeczi B., Gyógyszertechnológia 1., Medicina, Budapest (2001) p. 593.

[114] H. A. Liebermann, L. Lachmann, Pharmaceutical dosage forms: Tablets, Dekker 3 (1982) pp. 340-374.

[115] Marton S., Csóka G., Rácz I, Gyógyszerészet, 46 (2002) 680-683.

[116] Stability Testing of New Active Substances and Medicinal Products (ICH Q1A) (1993)

[117] H. C. Bülau, J. Ulrich, CGOM, ed. J. Ulrich, Shaker Verlag, Aachen (1997) 123-130.

[118] J. Ulrich, B. Kallies, Chemische Technik, 46 (1994) 229-234.

[119] E. Pallagi, P. Szabó-Révész, T. Haasner, M. Pásztor-Turák, O. Laczkovich, J. Ulrich, I. Erős, Pharm. Ind., 66 (2004) 112-117.

[120] T. Hassner, J. Ulrich, E. Pallagi, P. Szabó-Révész, Verfahrenstechnik, 35 (2001) 34-39.

[121] A. R. Rashid, J. Heinamöki, O. Antikainen, J. Ylirunsi, Drug Dev. Ind. Pharm. 25 (1999) 605.

[122] L. Shargel, A. Yu (Eds.), Applied Biopharmaceutics and Pharmacokinetics: Bioavailability and Bioequivalence, Appleton and Lange, USA (1999) pp. 247-279.

[123] Laczkovich O., Révész P., Pallagi E., Erős I., Acta Pharmaceutica Hungarica, 73 (2003) 243-248.

[124] Pallagi E., Szakdolgozat, Szeged (2001)

[125] Y. Qiu, N. Chindabaram, K. Flood, J. Control. Release., 51 (1998) 123-130.

Acknowledgement

First of all I would like to thank

Professor Dr. István Erős

Head of Department of Phramaceutical Technology for providing the possibility to complete my work under his advice.

My sincere thanks go to

Professor Dr. Piroska Szabó-Révész

whose valuable assistance in the practical work and during my complete research gave me useful advice and a lot of help.

I express my grateful thanks to

Professor Dr. Joachim Ulrich

Head of Department of Process Engineering, Martin-Luther University, Halle-Wittenberg, for providing the possibility to do scientific research in his department. Thanks for his advice and instructions.

I express my grateful thanks to my co-authors:

Prof. Dr. Klára Hódi, Prof. Dr. György Falkay, Dr. Klára Vass, Dr. Mónika Pásztor-Turák, Dr. Béla Farkas, Dr. Torsten Haasner and Dr. Péter Kása Jr.

for their co-operation.

I thank all members of the department for their help and friendship.

I owe my thanks to my family, my husband and friends for their support, encouragement and understanding attitude during these years.

ANNEX
Related articles